The type VII secretion system protects *Staphylococcus aureus* against antimicrobial host fatty acids

Arnaud Kengmo Tchoupa[a], Rebekah A. Jones[a], Agnès Kuroki[b], Mohammad Tauqeer Alam[a], Sebastien Perrier[a,b,c], Yin Chen[d], and Meera Unnikrishnan[a,1]

[a]Warwick Medical School, University of Warwick, Coventry CV4 7AL, United Kingdom; [b]Department of Chemistry, University of Warwick, Coventry CV4 7AL, United Kingdom; [c]Faculty of Pharmacy and Pharmaceutical Sciences, Monash University, 381 Royal Parade, Parkville, Victoria 3052, Australia; and [d]School of Life Sciences, University of Warwick, Coventry CV4 7AL, United Kingdom

[1]To whom correspondence should be addressed. Meera Unnikrishnan, Microbiology and Infection Group, Division of Biomedical Sciences, Warwick Medical School, University of Warwick, Coventry CV4 7AL, United Kingdom,
Email: M.Unnikrishnan@warwick.ac.uk.

Abstract

The *Staphylococcus aureus* type VII secretion system (T7SS) exports several proteins that are pivotal for bacterial virulence. The mechanisms underlying T7SS-mediated staphylococcal survival during infection nevertheless remain unclear. Here we show that EsxC, a small secreted effector implicated in bacterial persistence, contributes to *S. aureus* membrane architecture and fluidity. Interestingly, isogenic mutants lacking EsxC, other T7SS effectors (EsxA and EsxB) or the membrane-bound ATPase EssC are more sensitive to killing by the host-derived antimicrobial fatty acid, linoleic acid (LA), compared to the wild-type. We demonstrate that LA induces more cell membrane damage in the T7SS mutants, although they do not bind differentially to LA. Membrane lipid profiles show that T7SS mutants are also less able to incorporate LA into their membrane phospholipids. Proteomic analyses of wild-type and mutant cell fractions reveal that, in addition to compromising membranes, T7SS defects readily induce bacterial stress and hamper their response to LA challenge. Together, our findings indicate that T7SS is crucial for *S. aureus* membrane integrity and homeostasis, which is critical when bacteria encounter antimicrobial fatty acids.

Keywords: *Staphylococcus aureus*, Type VII secretion system, long-chain unsaturated free fatty acids.

Significance

Staphylococcus aureus is a major hospital and community-acquired pathogen that can cause a range of serious infections. Paradoxically, *S. aureus* is a common commensal inhabitant of skin and nares of healthy individuals, where the bacterium overcomes colonisation barriers deployed by the innate immune system, which include antimicrobial, unsaturated fatty acids (FAs). These long chain unsaturated free FAs are potent activators of the type VII secretion system (T7SS), a molecular machine that secretes virulence factors that promote *S. aureus* persistence in its host. Here we demonstrate a role for the T7SS in maintaining staphylococcal membrane architecture, which enables the bacteria to survive FA toxicity. An increased vulnerability to FAs might explain why T7SS-defective mutants are less virulent in FA-rich environments. Thus, therapeutics targeting the T7SS may mitigate *S. aureus* virulence and render the bacterium more susceptible to FAs.

Introduction

Staphylococcus aureus is a facultative pathogen that can colonize the skin and nares of healthy individuals. The asymptomatic carriage of *S. aureus* is a major risk for subsequent infections [1]. *S. aureus* infections, which are either health-care or community associated, range from benign impetigo to life-threatening bacteraemia and endocarditis [2]. Clinical management of staphylococcal infections is complicated by the increasing prevalence of multidrug resistant strains [3].

The success of *S. aureus* as a deadly pathogen is attributed to an array of virulence factors that enables it to strongly adhere to host tissues and evade immune responses [4]. One of these virulence factors is the type VII secretion system (T7SS), also known

as the ESAT-6 secretion system (ESS). The orthologous ESX-1 system was initially discovered in *Mycobacterium tuberculosis*, where it is essential for bacterial virulence [5]. T7SSs are found in both Gram-positive and Gram-negative bacteria (T7SSb), although these systems and their secretion machineries appear to be distinct to their mycobacterial counterparts [6].

Essential components of *S. aureus* T7SS are highly conserved, contrasting with the high variability within this secretion machinery [7]. In strains where it has been extensively studied (COL, RN6390, USA300 and Newman), the T7SS is similar and consists of four integral membrane proteins (EsaA, EssA, EssB and EssC), two cytosolic proteins (EsaB and EsaG), 5 secreted substrates (EsxA, EsxB, EsxC, EsxD and EsaD), and EsaE, which interacts with the T7SS substrates to target them to the secretion apparatus [8]. More recently, a peptidoglycan hydrolase, EssH, which allows T7SS transport across the bacterial cell wall envelope, was identified in USA300 [9].

The molecular architecture of the staphylococcal T7SS has not yet been fully characterized. T7SS integral membrane proteins EsaA, EssA, EssB, and EssC are thought to be the core of the T7 secretion machinery, with EssC being the central membrane transporter [10-12]. Interactions between secreted substrates and co-dependent secretion of substrates have been demonstrated [8, 13-15]. Recently, the functional assembly of the type VII secretion machinery, in *S. aureus*, was reported to be supported by the flotillin homolog FloA within the functional membrane microdomains [16].

S. aureus T7SS has been strongly linked to bacterial virulence since its discovery [17]. More specifically, *S. aureus* mutants unable to secrete EsxA or EsxB were defective in their ability to form kidney abscesses in a murine infection model [10]. In the same

mouse infection model, EsaB, EsxC, and EsaD were then shown to be required for *S. aureus* persistence [18, 19]. Likewise, in a murine pneumonia model, deletion of the whole T7SS in both strains RN6390 and COL led to reduced nasal colonisation and increased survival of infected mice [14]. In addition, in a *S. aureus* strain from a different lineage, ST398, T7SS was associated with increased virulence and epidemiological success [20].

Mechanisms by which T7SS effectors modulate host-bacterial interactions are multifaceted and not yet fully understood. EsxA is necessary to delay apoptosis of *S. aureus*-infected epithelial cells, and EsxA overexpression in these cells is sufficient to mitigate staurosporine-induced apoptosis [21]. The anti-apoptotic effects of EsxA were confirmed with human dendritic cells, where EsxB is involved in regulating the production of regulatory and anti-inflammatory cytokines upon infection with *S. aureus* [22]. The production of cytokines is also altered in a bacteraemia murine model, when bacteria are deprived of EsaD or EsaE [15, 23]. *S. aureus* ST398 T7SS and the newly discovered EsxX substrate contribute to bacterial replication inside human neutrophils, which are ultimately lysed [20, 24]. While less is understood about the relevance of T7SS to *S. aureus*, a role for the toxin-antitoxin pair EsaD (or EssD) and EsaG (or EssI) was demonstrated in intraspecies competition between *S. aureus* strains [8, 15].

S. aureus is known to tightly control the expression of its virulence factors in response to a range of environmental cues [25]. T7SS transcription is fine-tuned by intricate regulators, which comprise the alternative sigma factor σ^B, the global virulence regulator Agr, and the SaeRS two-component regulatory system [13, 20, 26]. T7SS expression is downregulated in human whole blood [27], and reduced by *S. aureus* inside polymorphonuclear neutrophils [28] in order to survive microbicidal azurophilic

granule proteins [29]. In contrast, calf-derived pulmonary surfactant, human blood serum and nasal secretions are potent stimulators of T7 secretion [30, 31].

Interestingly, *S. aureus* T7SS expression is induced in response to host-specific fatty acids [30-32], but the role of T7SS in bacterial resistance to antimicrobial fatty acids remains unclear. In this study, we demonstrate that *S. aureus* mutants, which lack the T7SS substrate EsxC have a defective cell membrane. Intriguingly, these and other T7SS mutants were more sensitive to an unsaturated fatty acid, linoleic acid (LA), compared to the wild-type strain. Although there were no differences in direct binding of LA to the T7SS mutants, LA induced a more leaky membrane in the T7SS mutants. Cellular proteomics revealed that in addition to membrane discrepancies, T7SS mutants exhibited different redox and metabolic states, which led to a markedly distinct response to LA.

Results

The type VII secreted substrate EsxC alters the staphylococcal membrane architecture

EsxC, a small 15-kDa protein secreted by the T7SS, is important for the persistence of *Staphylococcus aureus* in mice [18]. However, mechanisms underlying EsxC- or T7SS-mediated bacterial survival are not known. In order to understand the role of EsxC, we generated an isogenic *esxC* mutant as described previously [33], and confirmed the absence of any secondary site mutations by whole genome sequencing. Δ*esxC* had a similar growth rate to the wild-type (WT) USA300 JE2 strain (Fig. S1). Intriguingly, when imaged under a fluorescent microscope after staining with the membrane dye FM 4-64, Δ*esxC* was defective in staining compared to WT strain (Fig.

1A). This phenotype was reversed upon complementation of Δ*esxC* with a multicopy plasmid containing the *esxC* gene (Fig. 1A). FM 4-64 fluorescence intensity was quantified and revealed a clear, statistically significant ($P < 0.001$) difference between the WT and the mutant (Fig. 1B).

As differences in FM 4-64 staining suggest changes in the membrane structure, we probed this further by assessing membrane fluidity. We used pyrene decanoic acid, an eximer-forming lipid [31], to measure the fluidity of WT and Δ*esxC* membranes. Compared to the WT, the cytosolic membrane of the *esxC* mutant was slightly but consistently more rigid (Fig. 1C). These data indicate that EsxC contributes to *S. aureus* membrane architecture and fluidity.

EsxC is present on the staphylococcal surface and affects its composition.

As EsxC was initially reported to be secreted [18], it was surprising that this T7SS substrate would modulate the *S. aureus* membrane (Fig. 1). However, EsxC has been consistently detected in membrane fractions of RN6390 and USA300 strains [9, 14]. We were able to demonstrate the presence of EsxC in the membrane fractions of the WT USA300 JE2 strain but not in Δ*esxC* (Fig. 2A). Moreover, we also detected EsxC in the cell wall fraction from WT (Fig. 2A). To determine if the cell surface location of EsxC relies on a functional type VII secretion machinery, an isogenic mutant with a deletion of the membrane bound EssC protein (a core component of the T7SS) was generated. EsxC was still detected in cell membrane and cell wall preparations of the WT strain even in the absence of EssC (Fig. 2A).

To investigate if the absence of EsxC in both the membrane and the cell wall affects the bacterial cell surface, we treated intact bacteria (WT or Δ*esxC*) with trypsin to

digest surface proteins and analyse the cell surface proteome (surfome). Intriguingly, most of the detected proteins (172 out of 218) were less abundant in Δ*esxC* compared to the WT (Fig. 2B), with 20 proteins below the significance threshold ($P < 0.05$) (Table 1). Only three bacterial cell wall associated proteins were present at significantly higher levels in Δ*esxC* surfome: the surface protein G, the fibronectin-binding protein A (FnbA), and the secretory antigen (SsaA).

Surprisingly, the majority of proteins (16 out of 20) that were relatively less abundant in the *esxC* mutant surfome were predicted or proven to be cytosolic (Table 1). Proteins that were lowest in abundance (fold change < 0.5) were either metabolic (PfKA, FolD, FabI GatB, and ImdH) or stress-related (Asp23 and putative universal stress protein) (Fig. 2B). The other less abundant proteins (4) were the uncharacterised secreted protein A0A0H2XFG6, the iron-regulated surface determinant protein A IsdA, the putative lipoprotein A0A0H2XH82, and the membrane bound, T7SS core component EsaA. Indeed, EsaA, which has a prominent extracellular loop [34], was ~50% less abundant in Δ*esxC*, implying that EsxC absence may affect the T7SS assembly or display.

Consistent identification of cytosolic proteins during *S. aureus* surfome analyses may be due to non-canonical secretion of cytosolic proteins that can bind to bacterial surfaces [35, 36] or cell lysis during sample preparation [34, 37, 38]. However, the reduction in cytosolic proteins and the increased levels of SsaA that we observed in Δ*esxC* were similar to what was previously described for a mutant deficient in the major autolysin Atl [36]. Therefore, we compared autolysin-dependent Triton X-100 lysis of WT, Δ*esxC* and, Δ*essC*, a mutant lacking the major ATPase EssC required for T7SS export, in PBS (non-growing conditions). While Δ*esxC* was slightly more resistant to Triton X-100 (less prone to autolysis), Δ*essC* was clearly defective in

autolysis (Fig. 2C and D), as compared to the WT. Together, our data strongly suggest that the presence of EsxC in the cell envelope contributes to shaping the bacterial surface.

S. aureus _esxC_ and _essC_ mutants are more sensitive to linoleic acid.

S. aureus has been consistently shown to substantially augment the levels of T7SS expression, when grown in presence of host fatty acids [30-32]. Given our findings that the *esxC* mutant has a defective cell membrane and that *esxC* deletion affects the surface abundance of IsdA, which is essential for *S. aureus* resistance to antimicrobial fatty acids [39], we grew WT USA300 JE2 and its isogenic *essC* or *esxC* mutant in the presence of an unsaturated fatty acid (C18:2), linoleic acid (LA), at a concentration (80 μM) that still allows WT growth. Bacteria were also grown in parallel in presence of stearic acid (SA), a saturated C18:0 fatty acid. The T7SS mutants displayed impaired growth in presence of LA but not SA, as measured by optical density (Fig. 3A) or colony forming units (Fig. 3B). Importantly, Δ*esxC* complemented with a plasmid containing the *esxC* gene reverted to the WT phenotype (Fig. 3C).

T7SS substrates contribute to _S. aureus_ resistance to LA toxicity.

Next, we investigated whether T7SS proteins other than *essC* and *esxC* contributed to *S. aureus* growth in presence of LA. Mutants lacking two other substrates, Δ*esxA* and Δ*esxB*, were grown in presence of fatty acids. Again, mutations affecting these T7SS components caused bacteria to replicate slower than the WT USA300 (Fig. 4A). To ensure that the increased sensitivity observed for the T7SS mutants was not strain specific, RN6390 Δ*essC* or Δ*esxC* and Newman Δ*esxA* or Δ*esxB* mutants were tested.

Similar to USA300 mutants, the growth of these T7SS mutants was also impacted in the presence of LA (Fig. 4B and 4D). The growth defect in Newman Δ*esxA* was abrogated upon complementation (Fig. 4C). Of note, Newman WT was readily inhibited by only 40 μM LA. This is in agreement with the lower expression levels of the T7SS in this strain compared to USA300 [13, 14]. We conclude that a functional T7SS plays a role in *S. aureus* resistance to LA toxicity.

T7SS does not affect bacterial affinity to LA, but is required for maintaining membrane integrity upon LA binding.

As our membrane studies and surfome analyses strongly suggested that the bacterial envelope is altered upon T7SS defect, we hypothesised that LA-mediated growth inhibition of T7SS mutants was due to an increased binding to LA. To test this hypothesis, we chemically engineered LA to produce an azide functionalised LA (N^6-diazo-N^2-((9Z,12Z)-octadeca-9,12-dienoyl)lysine, N_3-LA) or azide-LA (Fig. 5A). After incubating bacteria with azide-LA, click-chemistry with an alkyne dye (Click-iT™ Alexa Fluor™ 488 sDIBO alkyne) was used to stain azide-LA associated with bacteria. There were no obvious differences in the fluorescence from *essC* and *esxC* mutants compared to the WT (USA300 JE2) (Fig. 5B), suggesting that T7SS components are not involved in binding or sequestering LA. However, when bacteria treated with azide-LA were stained with propidium iodide (PI), a good indicator of membrane integrity, Δ*essC* and Δ*esxC* displayed a more intense PI staining in comparison the WT (Fig. 5C and D). This suggests that an intact T7SS helps *S. aureus* to maintain its membrane integrity when faced with the detergent-like effects of unsaturated fatty acids.

Incorporation of LA into membrane phospholipids is compromised in the absence of T7SS.

Our findings that T7SS mutants have a compromised membrane, which responds differently to LA, led us to investigate the contribution of membrane lipids to these phenotypes. Lipids from WT (USA300 JE2) and T7SS mutants were analysed by high-performance liquid chromatography (HPLC)-mass spectrometry (MS) in negative ionisation mode. In keeping with previous reports [40, 41], phosphatidylglycerol (PG) was the major phospholipid present in the membrane of WT grown in TSB (Fig. S2A). Δ*essC* and Δ*esxC* grown with or without 10 μM LA [(a concentration that has been previously shown to be sub-inhibitory for USA300 [31]] displayed lipid profiles similar to that of WT (Fig. S2A and B). Notably, PG molecular species were significantly altered upon growth in LA-supplemented TSB for WT (Fig. 6A), Δ*essC* (Fig. S3) and Δ*esxC* (Fig. 6B). Three new LA-specific PG species with mass to charge ratios (m/z) 731 (C33:2), 759 (C35:2), and 787 (C37:2) appeared to contain LA (C18:2) or its elongated C20:2 or C22:2 versions, as revealed by their fragmentations (Fig. S4). These PG species containing exogenous, unsaturated FAs were also present in Δ*essC* and Δ*esxC*. However, LA (C18:2)-containing PG species (C33:2) was less abundant in the *esxC* mutant compared to WT (Fig. 6C). A similar trend, although statistically non-significant ($P > 0.05$), was observed for C20:2- and C22:2-containing PG species (Fig. S5), and when all the unsaturated exogenous PG species were combined (Fig. 6D). We conclude that a T7SS defect may compromise the incorporation and elongation of LA in *S. aureus* membranes.

T7SS mutations affect the total cellular content and the response of *S. aureus* to LA.

In order to gain further insight into mechanisms underlying T7SS action in presence of LA, we used an unbiased proteomic approach to study protein profiles of WT strain (USA300 JE2) and isogenic *essC* or *esxC* mutants grown exponentially with or without 10 μM LA. Interestingly, Δ*essC* or Δ*esxC* cultured in TSB readily displayed proteins with changed abundance when compared to the WT, with 37 and 24 proteins significantly ($P < 0.05$) altered in Δ*essC* and Δ*esxC*, respectively. Similarly, 14 proteins were differentially abundant in both *essC* and *esxC* mutants (Fig. 7A and B). These included proteins involved in signal transduction (LytR and ArlR), cell wall composition (acetyltransferase GNAT, FnbB and MazF), DNA repair (MutL and RadA), nucleotide binding (ATP-grasp domain protein and YqeH), hydrolysis (amidohydrolase), cell stress response (universal stress protein (Usp) family), or uncharacterised (A0A0H2XGJ8, YbbR and lipoprotein) (Fig. 7B and Table 2). Of the 33 proteins that were only changed in Δ*essC* (23) or Δ*esxC* (10), nearly 40% (13) associated with oxidation-reduction and other metabolic processes. Ten membrane proteins were more abundant in the absence of EssC (Table 2), which included SrrB, a membrane protein, whose gene expression was shown to be increased 6 times upon growth of USA300 in presence of LA [31]. SrrB was also detected at higher levels in the *esxC* mutant although the increase was non-significant ($P = 0.07$).

Next, we compared the proteomic profiles of LA-treated strains (WT, Δ*essC* or Δ*esxC*) with their untreated counterparts. Clearly, the principal component analysis revealed that the differences due to the genetic makeup (WT or T7SS mutants) were less prominent than the dramatic changes induced by LA (Fig. S6). These changes are exemplified for the WT; out of 1132 proteins identified, 163 proteins with an altered

relative abundance upon growth with LA (Fig. 7C). 167 and 171 proteins were changed ($P < 0.05$) in Δ*essC* and Δ*esxC*, respectively, in response to LA, of which ~ 40% (68) were common to these mutants and their WT (Fig. 7D). At least 30% of the significantly changed proteins ($P < 0.05$) were unique to WT (53), Δ*essC* (50), or Δ*esxC* (64) (Fig. 7D), suggesting that each strain responds differently to LA. However, all but one protein (13/14) that were similarly deregulated in *essC* and *esxC* mutants grown without LA (Fig. 7B) are modulated in presence of LA (highlighted in bold in Table S1). Proteins that were less abundant in both mutants were, upon LA treatment, either increased to WT levels (MutL, acetyltransferase GNAT, Toxin MazF, and ATP-grasp domain protein), or were unchanged in the mutants and decreased in the LA-treated WT (LytR and FnbB) [Table S1]. Likewise, proteins with increased amounts upon *essC* or *esxC* deletion were: (i) downregulated to WT levels in response to LA (putative lipoprotein A0A0H2XGW7), (ii) unaltered in both mutants and upregulated in WT (Usp, amidohydrolase, and YbbR), (iii) or further increased in the *essC* mutant and strongly upregulated in WT (A0A0H2XGJ8) [Table S1]. In sum, except for ArlR and RadA that were conversely regulated in WT and the T7SS mutants after LA treatment, proteins similarly deregulated upon *esxC* or *essC* deletion were returned to similar levels in response to LA. A similar trend was observed for 15 out of 23 and all the 10 proteins exclusively more or less abundant in Δ*essC* and Δ*esxC*, respectively.

We then used QuickGO (a web-based tool for Gene Ontology searching) [42] to retrieve GO terms associated with the ten most significantly upregulated proteins in WT upon LA treatment (Table S1). Strikingly, 9/10 of these proteins had a hydrolase or an oxidoreductase activity. A comprehensive, statistical analysis to determine if specific molecular functions were significantly enriched in response to LA showed a clear enrichment of 8 molecular functions ($P < 0.05$) in at least one strain (WT or T7SS

mutants) (Fig. 7E). Oxidoreductase and hydrolase activities were enhanced in LA-treated WT, while Δ*essC* and Δ*esxC* were less able to upregulate proteins with these molecular functions. Flavin adenine dinucleotide (FAD)-binding, which is also involved in oxidation-reduction and fatty acid metabolic processes, was similarly more enriched in LA-WT. In contrast, transferase activity, which is linked to cell wall synthesis, was induced more in T7SS mutants compared to the WT.

We also determined the molecular functions that are decreased upon LA challenge (Fig. 7F). In agreement with reduced intracellular ATP levels following membrane damage by antimicrobial fatty acids [43], USA 300 JE2 WT strongly inhibited genes with the ATP binding function (mainly ATP-binding ABC transporters). The ATP-dependent lyase activity was also repressed by the WT. T7SS mutants, on the contrary, were less able to modulate ATP-binding proteins and instead relied on a strong inhibition of ribosomal constituents as well as other components of translation in general (Fig. 7E). Taken together, our proteomic analyses reveal that the lack of T7SS induces altered membrane and metabolic states, reminiscent of oxidative stress responses. While the WT shows a multifaceted response to mitigate the damages caused by LA on the bacterial membrane, these responses are clearly altered when T7SS is compromised.

Discussion

Host fatty acids (FAs) play a crucial role in the host defence to *S. aureus* infections. *S. aureus* is particularly sensitive to unsaturated FAs, which are abundant in the human skin [39, 44]. We report here that the T7SS, an important component of *S. aureus* virulence arsenal, is critical in modulating the response to antimicrobial host FAs by

maintaining the bacterial cell membrane integrity. Specifically, we demonstrate that a T7SS substrate, EsxC, impacts *S. aureus* membrane properties, presumably by altering T7SS assembly. A functional T7SS enables bacteria to mitigate LA-induced toxicity and grow better than mutants with a compromised T7SS. In the absence of T7SS components, LA enhances cell membrane damage, and cellular proteomics suggest that bacteria are readily stressed and unable to activate adaptive mechanisms involved in the resistance to LA.

Although several recent studies have revealed multiple interactions between the staphylococcal T7SS components, the precise molecular architecture of this system remains largely unknown. Burts and co-authors first described the 15-kDa EsxC (previously EsaC), as a secreted protein, whose secretion was abrogated upon deletion of *essC*, the central T7SS transporter in *S. aureus* [18]. Further evidence of EsxC being a T7SS substrate is the impaired production and/or secretion of the cognate T7SS substrates EsxA and EsxB in absence of EsxC [13]. Indeed, for EsxA-D, EsaD (EssD) and EsaE (EssE), the deletion of one of these T7SS effectors affects the stability and/or the successful export of others T7SS substrates, although such effects appear to be strain-dependent [8, 10, 13-15, 18, 19, 23]. EsaE was reported to partially localize in *S. aureus* membranes and interact with membrane-bound EssC, EsxC, EsaD and EsaG [8, 23]. In *esaE* defective mutants, less EsxB and EsxD were detected in whole cell lysates, while EsxA, EsxB, EsxC and EsxD were drastically reduced in bacterial supernatants [23]. As reported previously, we also found that EsxC can localize within staphylococcal membranes [9, 14]. Thus, based on available data, EsxC is likely to be associated to EsxA, EsaD, or EsaE on the membrane [13, 23]. However, the reduced EsaA protein levels that we found on the surface of *S. aureus* USA300 JE2 Δ*esxC* combined with prior observations of diminished EsxC

protein levels in the membrane of a RN6390 *esaA* mutant [14] suggest that EsxC may interact with EsaA in *S aureus* membranes. Since EsaA can strongly bind to EssB, and EsaA-EssB complexes assemble to polymeric structures comprising EssA, EssC, EsaD and EsxA [45], it is enticing to speculate that EsxC is part of the T7SS machinery, and not just a secreted substrate. This is in agreement with a previous report that EsxA secretion in USA300 is abrogated upon *esxC* deletion [13].

Recently, the functional membrane microdomain (FMM) protein flotillin was shown to play a key role in assembly of the staphylococcal T7SS. Mielich-Suss and co-workers reported that T7SS integral membrane proteins like EssB are not evenly distributed in *S. aureus* membranes, but interact with the flotillin homolog FloA within FMMs [16]. Well-structured FMMs might play a role in membrane fluidity of *S. aureus* as they do for *Bacillus subtilis* [46]. Interestingly, *S. aureus* T7SS transcripts were reported to be more abundant, when there was a reduction of membrane fluidity [31]. Furthermore, in a *S. aureus* mutant lacking *fakA*, which displays increased membrane rigidity [31], T7SS genes are upregulated in comparison to the isogenic WT strain [47]. Detergents, which affect staphylococcal membrane, also stimulate the T7SS [30]. Hence, there appears to be a link between membrane fluidity and T7SS in *S. aureus*, and it was suggested that the membrane state triggers the production of T7SS [31]. Remarkably, we find that *esxC* deletion led to a reproducible mild increase in bacterial membrane rigidity and membrane defects (Figs. 1 and 2), suggesting membrane modulation by the T7SS. It is plausible that interactions between FloA and T7SS are perturbed enough upon *esxC* deletion to affect *S. aureus* FMMs. We surmise that a functional T7SS helps *S. aureus* to maintain its membrane architecture.

The current cellular proteomics data reveal that, in comparison to *S. aureus* USA300 JE2 WT, the deletion of *essC* alters the abundance of higher number of proteins (37)

than that of *esxC* (24). This is in keeping with the greater importance of EssC as the conserved driving force of the T7SS [7]. Importantly, almost 60% of proteins deregulated in Δ*esxC* are similarly affected in Δ*essC*, strongly suggesting that any modification of the T7SS core leads to a similar staphylococcal response. Likewise, in the strain RN6390, most genes that were dysregulated in Δ*essC* were similarly altered in the *esaB* mutant [48]. However, surprisingly, proteins with altered abundance in USA300 Δ*essC* do not correspond to differentially expressed genes in RN6390 Δ*essC* [49]. This apparent discrepancy might be due to differences in strains. Nevertheless, the upregulation in RN6390 Δ*essC* of genes under the control of the ferric uptake regulatory protein Fur, which was shown not to be due to iron-starvation [49], might indicate an altered oxidative status following *essC* deletion given the known role of Fur in oxidative stress resistance [50, 51]. Our proteomics data reveal that many proteins with oxidoreductase activity were more abundant in USA300 JE2 Δ*essC*. *S aureus* RN6390 was also shown to differentially express redox-sensitive genes in absence of EsaB [48]. Since the T7SS substrate EsxA is upregulated in response to hydrogen pyroxide [49], one could speculate that lack of T7SS stimulate an oxidative stress response that might be an indirect effect of the membrane destabilization.

A further indication of altered physiological states of Δ*essC* and Δ*esxC* was the changed abundance of proteins belonging to the two-component regulatory systems LytSR, ArlSR and SrrAB (LytR, ArlR, and SrrB, respectively). LytR and ArlR protein levels were decreased in both *essC* and *esxC* mutants, consistent with a previous report of the down-regulation of *lytR* transcription in absence of *arlR* [52]. LytRS can: (i) modulate the bacterial surface [53], (ii) monitor membrane potential changes [54], and (iii) affect biofilm formation [55], whereas SrrAB can sense and respond to impaired electron flow in the electron transport chain [56]. Importantly, the *S. aureus*

response to antimicrobial FAs includes downregulation of *lytRS* [32, 57], and upregulation of *srrB* [31]. As LytR and SrrB levels were altered in Δ*essC* or Δ*esxC* in comparison to WT, impairments of the T7SS are likely to result in a changed cell envelope, which impacts how bacteria respond to the LA challenge.

Antimicrobial free FAs such as LA are known to target bacterial membranes [58]. LA and other unsaturated FAs that are not produced by *S. aureus* can, however, be used by this bacterium for its phospholipid synthesis via a two-component fatty acid kinase (Fak) [44, 47, 59]. Exogenous FAs are bound by FakB1 if saturated or FakB2 if unsaturated [47]. FakB-bound FAs are phosphorylated by FakA to generate acyl-PO4, which can be incorporated into membrane phospholipids [47]. Nonetheless, *S. aureus* growth is inhibited by LA *in vitro* [32, 60, 61]; strikingly, the T7SS is strongly upregulated when *S. aureus* is grown in presence of sub-inhibitory concentrations of LA [31, 32]. Furthermore, Lopez and co-workers, by carefully examining the structure-activity relationships of a panel of long-chain fatty acids, discovered that fatty acids with more cis double bonds, which are more toxic toward *S. aureus* [44], are also more potent T7SS activators [31]. Our current study demonstrates that *S. aureus* mutants with a defective T7SS grow slower in the presence of LA, which strongly suggests a protective role of T7SS against LA toxicity. But how does the T7SS mediate this protective effect? The previously identified resistance mechanisms to antimicrobial fatty acids (AFA) in *S. aureus* include: (i) modulation of cellular hydrophobicity by the surface protein IsdA or wall teichoic acids [39, 44, 62, 63], and (ii) AFA detoxification with the efflux pumps Tet38 and FarE [64, 65]. Surprisingly, our proteomic analyses revealed that IsdA was less abundant in the LA-treated WT, and no significant changes were seen in the mutants. As other proteins affecting cell wall organisation (IsdH, sortase A, Pbp3, and TarK) were also inhibited in response to LA, this might be

due to a major restructuring of the cell wall when *S. aureus* is grown in presence of LA. Thus, previously described resistance mechanisms do not appear to explain why T7SS mutants are more susceptible to LA.

Our data suggest that the preservation of staphylococcal membrane architecture is also crucial in the response to LA. A role for the T7SS in cell membrane homeostasis is further supported by the activation of staphylococcal T7SS by membrane-modifying factors such as detergents and temperature (30, 31). Indeed, T7SS mutants, which appeared to bind LA similarly, displayed an increased membrane permeability upon LA binding and were less able to incorporate LA into their phospholipids. However, the observation that this LA incorporation was impacted more in Δ*esxC* than in Δ*essC* seems counterintuitive given the central role of EssC in T7 secretion [10-12]. This might indicate that secretion per se is not required for LA incorporation; EsxC accumulated in the membrane (Fig. 2A) could mediate LA incorporation in the *essC* mutant. It is also worth noting that transcript levels of *esxC*, and not *essC*, were strongly upregulated in a *S. aureus fakA* mutant [47]. Levels of FakA, FakB1 and FakB2 showed no changes in the T7SS mutants in presence or absence of LA, suggesting no regulatory control of the Fak pathway by the T7SS. Hence, we speculate that EsxC and other interdependent T7SS substrates play an important role in facilitating Fak function in *S. aureus* membranes, either by mediating recruitment or correct targeting of Fak proteins to the membrane. Our findings warrant further investigations into molecular mechanisms underlying T7SS-mediated FA incorporation within staphylococcal membranes.

The growth of *S. aureus* USA300 JE2 WT in presence of LA increases the levels of the T7SS proteins EsxA and EsaA, the oleate hydratase McrA, and the staphylococcal respiratory response protein SrrB, in keeping with prior gene expression analyses [31,

32]. Furthermore, WT membranes showed major remodelling upon LA-treatment. Specifically, increased levels of cytochrome D ubiquinol oxidase subunit I and SrrB point to a perturbation of respiration. Another AFA, sapienic acid, has been previously reported to inhibit respiration [43]. On the whole, *essC* and *esxC* mutants seem to display similar metabolic and structural responses to LA compared to the WT. However, both T7SS mutants were less able to further prime their redox-active proteins. Instead, to cope with LA, they appear to rely on strong inhibition of the protein synthesis machinery, which is reminiscent of the stringent response [66].

Taken together, we conclude that T7SS plays a key role in modulating the *S. aureus* cell membrane in response to toxic host fatty acids. We propose that the increased susceptibility of T7SS mutants to LA might explain why they are less virulent in LA- and other AFA-rich environments like the mouse lungs (Δ*essC*) [30], abscesses (Δ*esxC* and Δ*esaB*), liver and skin (Δ*essB*) [20, 31]. Previous research has shown that T7SS induction by host-derived fatty acids is a fine-tuned activation of environment-specific bacterial virulence factors [30, 31]. Although, at present, it is still unclear how T7SS contributes to staphylococcal membrane architecture, T7SS interaction with the flotillin homolog FloA within functional membrane microdomains [16] supports the idea that T7SS proteins interact with many other proteins to modulate *S. aureus* membranes. Indeed, our data also suggest that blocking T7SS activity would make *S. aureus* more vulnerable to antimicrobial fatty acids, a key anti-staphylococcal host defence, thus making T7SS a very attractive drug target.

Materials and methods

Bacterial strains and growth conditions. The *S. aureus* strains used in this study are listed in the Table 3, and grown aerobically in tryptic soy broth (TSB) overnight (O/N) at 37ºC for each experiment unless stated otherwise. For complemented *S. aureus* strains, TSB was supplemented with 10 µg/mL chloramphenicol.

Construction of bacterial mutants. The primers used are listed in the Table 4. In-frame deletion of *essC* or *esxC* was performed as described previously [33]. Briefly, 1-kb DNA fragments up and downstream of the targeted gene sequence were PCR-amplified from USA300 LAC JE2 chromosomal DNA, and both PCR products fused via SOEing (splicing by overlap extension)-PCR. The 2-kb DNA fragment obtained was cloned into pKORI, and used for in-frame deletion. Putative mutants were screened by PCR-amplification of a fragment including the gene of interest, whose deletion was confirmed by Sanger sequencing. Further, to confirm that successful mutants did not have any additional mutations, Illumina whole genome sequencing was performed on libraries prepared with the Nextera XT kit and an Illumina MiSeq® instrument following manufacturers' recommendations. For complementation, full-length *esxC* gene was cloned onto pOS1CK described previously [21].

Membrane fluidity assay. O/N bacterial cultures were diluted to an OD_{600} of 0.15 in TSB, and were grown to an OD_{600} of 1 (OD1). Bacteria were washed with PBS prior to treatment for 30 min at 37ºC with 37.5 µg/mL lysostaphin in PBS containing 20% sucrose. The spheroblasts were then centrifuged at 8000 × *g* for 10 min, and the pellet resuspended in the labelling solution (PBS, 20% sucrose, 0.01% F-127, 5 µM pyrene decanoic acid). The incubation in the dark was done for 1h at 25ºC under gentle rotation. PBS supplemented with 20% sucrose was used to wash the stained

spheroblasts that were afterwards transferred to 96-well plates for fluorescence measurements as previously described [31].

Autolysis assays. Whole cell autolysis assays were performed as described elsewhere with a few modifications [67]. Specifically, OD1-grown *S. aureus* USA300 JE2 WT, *essC* and *esxC* mutants were extensively washed with PBS followed by ice-cold water, and resuspended in PBS with 0.1% Triton X-100 to an OD_{600} of 0.7. Subsequently, the samples were incubated with shaking at 37ºC for 2h, after which bacteria were diluted with PBS and plated for CFU determination.

Growth curves. O/N bacterial cultures were diluted to an OD_{600} of 0.05 in plain TSB or TSB supplemented with fatty acids. Bacteria were then grown in a 96-well plate with shaking, and the OD_{600} was measured every 15 minutes with a FLUOstar OMEGA plate reader (BMG Labtech, UK).

Cell shaving for surfome analysis. *S. aureus* USA300 JE2 WT grown to OD1 and Δ*esxC* were washed three times before being treated with Proteomics grade trypsin from porcine pancreas (Sigma-Aldrich, UK) for 15 min as described [37]. The samples were then centrifuged at 1000 × *g* for 15 min, and the bacterial pellets discarded while supernatants were filtered through a 0.2 µM filter. The freshly prepared peptides were frozen (-20ºC) until 2 additional, independent biological replicates per strain were prepared.

Cellular proteomics. *S. aureus* strains were grown O/N at 37ºC on tryptic soy agar plates. The next day, single colonies were used to inoculate 10 mL plain TSB or TSB with 10 µM LA. Cultures were grown at 37ºC with 180-rpm shaking until an OD_{600} of 3.2 ± 0.2 was reached. The bacteria were then centrifuged, washed with PBS, and resuspended in lysis buffer (PBS, 250 mM sucrose, 1 mM EDTA, and 50 µg/mL

lysostaphin) supplemented with cOmplete™, mini, EDTA-free protease inhibitor cocktail (Sigma-Aldrich, UK). After 15 min incubation at 37ºC, cells were lysed mechanically with silica spheres (Lysing Matrix B, Fischer Scientific, UK) in a fast-prep shaker as described previously [16]. Samples were then centrifuged, and the supernatants transferred to fresh tubes, where proteins were reduced and alkylated for 20 min at 70ºC with 10 mM TCEP (tris(2-carboxyethyl)phosphine) and 40 mM CAA (2-chloroacetamide), respectively. Next, the solvent was exchanged first to 8M urea buffer then to 50 mM ammonium bicarbonate. Proteins were digested O/N at 37ºC with mass spectrometry grade lysyl endopeptidase LysC and sequencing grade modified trypsin (Promega LTD, UK).

Label-free protein quantification. Peptides prepared for surfome or whole-cell proteome analyses were desalted and concentrated with a C18 cartridge in 40 µL MS buffer (2% acetonitrile plus 0.1% trifluoroacetic acid). For each sample, 20 µL were analysed by nanoLC-ESI-MS/MS using the Ultimate 3000/Orbitrap Fusion instrumentation (Thermo Scientific), and a 90 minute LC separation on a 50 cm column. The data were used to interrogate the Uniprot *Staphylococcus aureus* USA300 database UP000001939, and the common contaminant database from MaxQuant [68]. MaxQuant software was used for protein identification and quantification using default settings. Intensities were log_2-tansformed with the Perseus software, and proteins with one or no valid value for every sample in triplicate were filtered. For surfome data, the removeBatchEffect function of the limma R package [69] was used to remove differences accounting for variation in shaving efficiency done on three different days for all the biological replicates. Missing values in cellular proteomics data were imputed on R. Specifically, for each sample, the imputed value

was either the lowest intensity across all samples if at least two biological replicates had missing values or the average of two valid values if only one was missing.

Synthesis of azide functionalized linoleic acid. A 2-step synthesis was used to obtain N^6-diazo-N^2-((9Z,12Z)-octadeca-9,12-dienoyl)lysine, N_3-LA (azide-LA). LA was first functionalized with *N*-hydroxysuccinimide (NHS) in anhydrous dimethyl formamide (DMF) in presence of *N*-(3-dimethylaminopropyl)-*N'*-ethylcarbodiimide hydrochloride. The solvent was then removed and replaced by dicholoromethane (DCM), following which the reaction mixture was washed with water and dried over magnesium sulphate. The product, 2,5-dioxopyrrolidin-1-yl (9Z,12Z)-octadeca-9,12-dienoate (NHS-LA), was analysed using ^{1}H nuclear magnetic resonance (NMR) spectroscopy (Fig. S7A) and mass spectrometry (MS). MS: $[M+Na]^+$ 400.5 (calculated), 400.5 (found).

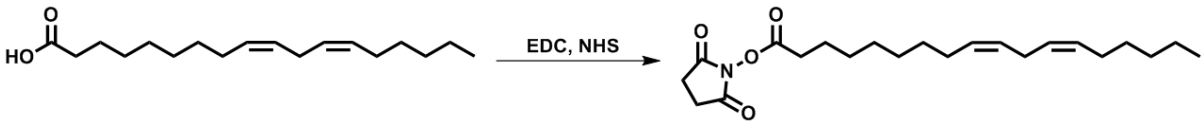

NHS-LA was left O/N at room temperature to react with L-azidolysine hydrochloride in anhydrous DMF, and produce azide-LA.

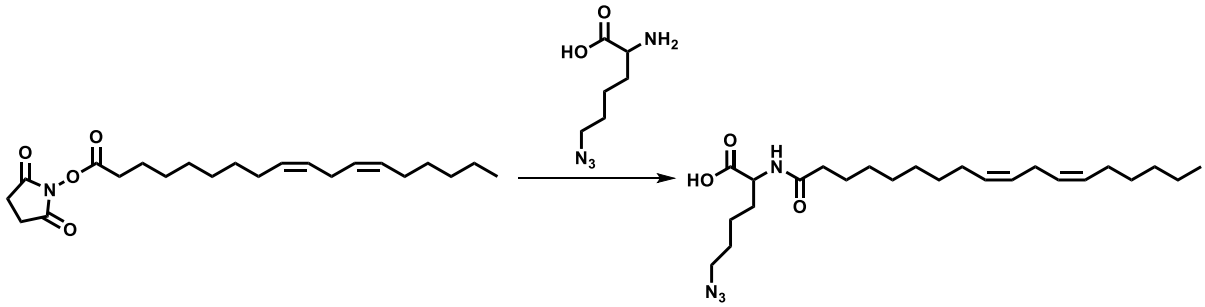

DMF was then removed, the reaction mixture precipitated in water, and dried under vacuum to obtain a clear oil. The composition of the oil was confirmed as being a mixture of azide-LA and unmodified LA (20% and 80%, respectively) based on ^{1}H

NMR (Fig. S7B) and MS data. MS: $[LA-H]^-$ 279.5 (calculated), 279.2 (found), $[M-H]^-$ 433.3 (calculated), 433.6 (found).

Binding assays with azide-LA and click chemistry. *S. aureus* USA300 JE2 WT, Δ*essC*, and Δ*esxC*, grown to OD1, were treated with 10 μM azide-LA for 15 min at 37ºC with shaking. The samples were then centrifuged, and the bacterial pellets resuspended in PBS supplemented with 4 μg/mL Click-iT™ Alexa Fluor™ 488 sDIBO alkyne (Life Technologies LTD, UK). After incubation at 25ºC for 1h with shaking, bacteria were washed with PBS, and binding to azide-LA was quantified by measuring fluorescence using a FLUOstar OMEGA plate reader (BMG Labtech, UK). The samples imaged with a microscope were additionally stained with 3 μM propidium iodide, following click chemistry.

Widefield microscopy. Bacteria stained with FM4-64 or Click-iT™ Alexa Fluor™ 488 sDIBO alkyne were immobilized on thin layers of agarose covering glass slides. Samples were then mounted using ProLong Gold Antifade Reagent with DAPI (New England Biolobs LTD, UK), and viewed with a Leica DMi8 widefield microscope (Leica Microsystems LTD, UK). Acquired images were analysed with the ImageJ processing package Fiji [70].

Lipid extraction and analyses. Lipids were extracted from bacterial cultures as described elsewhere [71]. Briefly, bacteria were grown to OD1 in TSB or TSB supplemented with 10 μM LA, centrifuged in a 2 mL glass Chromacol vial (Thermo Scientific), and resuspended in 0.5 mL MS grade methanol (Sigma-Aldrich). MS grade chloroform was then used to extract lipids. The extracted lipids were dried under nitrogen gas with a Techne sample concentrator (Staffordshire, UK), and the lipid pellets resuspended in 1 mL acetonitrile. The samples were then analysed by LC-MS

with a Dionex 3400RS HPLC coupled to an amaZon SL quadrupole ion trap mass spectrometer (Bruker Scientific) via an electrospray ionisation interface. Both positive and negative ionisation modes were used for sample analyses. The Bruker Compass software package was utilized for data analyses, using DataAnalysis for peak identification and characterization of lipid class, and QuantAnalysis for quantification of the relative abundance of distinct PG species to total PG species.

Statistical analyses. Except for the proteomics results, the statistical tests were performed with GraphPad Prism 8.0 as indicated in the figure legends, with *P* values < 0.05 considered significant. A paired two-tailed Student's t-test or a paired Mann-Whitney U test was used for pairwise comparisons. An ordinary one-way analysis of variance (ANOVA) with Dunnett's multiple comparisons test or a Kruskal-Wallis test with Dunn's multiple comparisons test was applied to data form three or more groups. The fold changes and *P* values of the proteomics data were calculated with the R package limma [69], with USA300 JE2 WT or bacteria grown without LA as references. These fold changes and *P* values were used by the R package piano [72] to compute the enrichment of gene ontology (GO) terms.

Acknowledgments

This study was supported by a Medical Research Council (MRC) grant (MR/N010140/1) to MU, an MRC Doctoral Training Partnership studentship in Interdisciplinary Biomedical Research (MR/J003964/1) awarded to RAJ, a CSIRO (Commonwealth Scientific and Industrial Research Organisation) scholarship to AK, and a Royal Society Wolfson Merit Award (WM130055) to SP. We thank Professor Tracy Palmer FRS (Institute for Cell and Molecular Biosciences, Newcastle University, UK) for the anti-EsxC serum, and the *S. aureus* strains RN6390 WT, RN6390 Δ*essC*

and RN6390 Δ*esxC*. We thank Professor Olaf Scheewind (Department of Microbiology, University of Chicago, Chicago, Illinois, USA) for providing us with the pOS1 and pKORI plasmids, and the *S. aureus* USA300 LAC and Newman strains. We thank GSK, Siena, Italy for providing the Newman *esxA*, *esxB* mutant strains used in this study. We acknowledge the contribution of the Proteomics Research Technology Platform, University of Warwick, UK.

References

1. von Eiff, C. et al. (2001) Nasal carriage as a source of *Staphylococcus aureus* bacteremia. Study Group. N Engl J Med 344 (1), 11-6.

2. Tong, S.Y. et al. (2015) *Staphylococcus aureus* infections: epidemiology, pathophysiology, clinical manifestations, and management. Clin Microbiol Rev 28 (3), 603-61.

3. Lee, A.S. et al. (2018) Methicillin-resistant *Staphylococcus aureus*. Nat Rev Dis Primers 4, 18033.

4. Gordon, R.J. and Lowy, F.D. (2008) Pathogenesis of methicillin-resistant *Staphylococcus aureus* infection. Clin Infect Dis 46 Suppl 5, S350-9.

5. Conrad, W.H. et al. (2017) Mycobacterial ESX-1 secretion system mediates host cell lysis through bacterium contact-dependent gross membrane disruptions. Proc Natl Acad Sci U S A 114 (6), 1371-1376.

6. Unnikrishnan, M. et al. (2017) The Enigmatic Esx Proteins: Looking Beyond Mycobacteria. Trends Microbiol 25 (3), 192-204.

7. Warne, B. et al. (2016) The Ess/Type VII secretion system of *Staphylococcus aureus* shows unexpected genetic diversity. BMC Genomics 17, 222.

8. Cao, Z. et al. (2016) The type VII secretion system of *Staphylococcus aureus* secretes a nuclease toxin that targets competitor bacteria. Nat Microbiol 2, 16183.

9. Bobrovskyy, M. et al. (2018) EssH peptidoglycan hydrolase enables *Staphylococcus aureus* type VII secretion across the bacterial cell wall envelope. J Bacteriol.

10. Burts, M.L. et al. (2005) EsxA and EsxB are secreted by an ESAT-6-like system that is required for the pathogenesis of *Staphylococcus aureus* infections. Proc Natl Acad Sci U S A 102 (4), 1169-74.

11. Jager, F. et al. (2018) EssC is a specificity determinant for *Staphylococcus aureus* type VII secretion. Microbiology 164 (5), 816-820.

12. Zoltner, M. et al. (2016) EssC: domain structures inform on the elusive translocation channel in the Type VII secretion system. Biochem J 473 (13), 1941-52.

13. Anderson, M. et al. (2013) Secretion of atypical protein substrates by the ESAT-6 secretion system of *Staphylococcus aureus*. Mol Microbiol 90 (4), 734-43.

14. Kneuper, H. et al. (2014) Heterogeneity in ess transcriptional organization and variable contribution of the Ess/Type VII protein secretion system to virulence across closely related *Staphylocccus aureus* strains. Mol Microbiol 93 (5), 928-43.

15. Ohr, R.J. et al. (2017) EssD, a Nuclease Effector of the *Staphylococcus aureus* ESS Pathway. J Bacteriol 199 (1).

16. Mielich-Suss, B. et al. (2017) Flotillin scaffold activity contributes to type VII secretion system assembly in *Staphylococcus aureus*. PLoS Pathog 13 (11), e1006728.

17. Pallen, M.J. (2002) The ESAT-6/WXG100 superfamily -- and a new Gram-positive secretion system? Trends Microbiol 10 (5), 209-12.

18. Burts, M.L. et al. (2008) EsaC substrate for the ESAT-6 secretion pathway and its role in persistent infections of *Staphylococcus aureus*. Mol Microbiol 69 (3), 736-46.

19. Anderson, M. et al. (2011) EsaD, a secretion factor for the Ess pathway in *Staphylococcus aureus*. J Bacteriol 193 (7), 1583-9.

20. Wang, Y. et al. (2016) Role of the ESAT-6 secretion system in virulence of the emerging community-associated *Staphylococcus aureus* lineage ST398. Sci Rep 6, 25163.

21. Korea, C.G. et al. (2014) Staphylococcal Esx proteins modulate apoptosis and release of intracellular *Staphylococcus aureus* during infection in epithelial cells. Infect Immun 82 (10), 4144-53.

22. Cruciani, M. et al. (2017) *Staphylococcus aureus* Esx Factors Control Human Dendritic Cell Functions Conditioning Th1/Th17 Response. Front Cell Infect Microbiol 7, 330.

23. Anderson, M. et al. (2017) EssE Promotes *Staphylococcus aureus* ESS-Dependent Protein Secretion To Modify Host Immune Responses during Infection. J Bacteriol 199 (1).

24. Dai, Y. et al. (2017) A Novel ESAT-6 Secretion System-Secreted Protein EsxX of Community-Associated *Staphylococcus aureus* Lineage ST398 Contributes to Immune Evasion and Virulence. Front Microbiol 8, 819.

25. Balasubramanian, D. et al. (2017) *Staphylococcus aureus* pathogenesis in diverse host environments. Pathog Dis 75 (1).

26. Schulthess, B. et al. (2012) Opposing roles of sigmaB and sigmaB-controlled SpoVG in the global regulation of esxA in *Staphylococcus aureus*. BMC Microbiol 12, 17.

27. Malachowa, N. et al. (2011) Global changes in *Staphylococcus aureus* gene expression in human blood. PLoS One 6 (4), e18617.

28. Voyich, J.M. et al. (2005) Insights into mechanisms used by *Staphylococcus aureus* to avoid destruction by human neutrophils. J Immunol 175 (6), 3907-19.

29. Palazzolo-Ballance, A.M. et al. (2008) Neutrophil microbicides induce a pathogen survival response in community-associated methicillin-resistant *Staphylococcus aureus*. J Immunol 180 (1), 500-9.

30. Ishii, K. et al. (2014) Induction of virulence gene expression in *Staphylococcus aureus* by pulmonary surfactant. Infect Immun 82 (4), 1500-10.

31. Lopez, M.S. et al. (2017) Host-derived fatty acids activate type VII secretion in *Staphylococcus aureus*. Proc Natl Acad Sci U S A 114 (42), 11223-11228.

32. Kenny, J.G. et al. (2009) The *Staphylococcus aureus* response to unsaturated long chain free fatty acids: survival mechanisms and virulence implications. PLoS One 4 (2), e4344.

33. Bae, T. and Schneewind, O. (2006) Allelic replacement in *Staphylococcus aureus* with inducible counter-selection. Plasmid 55 (1), 58-63.

34. Dreisbach, A. et al. (2010) Profiling the surfacome of *Staphylococcus aureus*. Proteomics 10 (17), 3082-96.

35. Hempel, K. et al. (2011) Quantitative proteomic view on secreted, cell surface-associated, and cytoplasmic proteins of the methicillin-resistant human pathogen *Staphylococcus aureus* under iron-limited conditions. J Proteome Res 10 (4), 1657-66.

36. Pasztor, L. et al. (2010) Staphylococcal major autolysin (Atl) is involved in excretion of cytoplasmic proteins. J Biol Chem 285 (47), 36794-803.

37. Solis, N. et al. (2014) *Staphylococcus aureus* surface proteins involved in adaptation to oxacillin identified using a novel cell shaving approach. J Proteome Res 13 (6), 2954-72.

38. Ventura, C.L. et al. (2010) Identification of a novel *Staphylococcus aureus* two-component leukotoxin using cell surface proteomics. PLoS One 5 (7), e11634.

39. Clarke, S.R. et al. (2007) The *Staphylococcus aureus* surface protein IsdA mediates resistance to innate defenses of human skin. Cell Host Microbe 1 (3), 199-212.

40. Delekta, P.C. et al. (2018) *Staphylococcus aureus* utilizes host-derived lipoprotein particles as sources of exogenous fatty acids. J Bacteriol.

41. Parsons, J.B. et al. (2011) Metabolic basis for the differential susceptibility of Gram-positive pathogens to fatty acid synthesis inhibitors. Proc Natl Acad Sci U S A 108 (37), 15378-83.

42. Binns, D. et al. (2009) QuickGO: a web-based tool for Gene Ontology searching. Bioinformatics 25 (22), 3045-6.

43. Cartron, M.L. et al. (2014) Bactericidal activity of the human skin fatty acid cis-6-hexadecanoic acid on *Staphylococcus aureus*. Antimicrob Agents Chemother 58 (7), 3599-609.

44. Parsons, J.B. et al. (2012) Membrane disruption by antimicrobial fatty acids releases low-molecular-weight proteins from *Staphylococcus aureus*. J Bacteriol 194 (19), 5294-304.

45. Aly, K.A. et al. (2017) Isolation of a Membrane Protein Complex for Type VII Secretion in *Staphylococcus aureus*. J Bacteriol 199 (23).

46. Bach, J.N. and Bramkamp, M. (2013) Flotillins functionally organize the bacterial membrane. Mol Microbiol 88 (6), 1205-17.

47. Parsons, J.B. et al. (2014) Identification of a two-component fatty acid kinase responsible for host fatty acid incorporation by *Staphylococcus aureus*. Proc Natl Acad Sci U S A 111 (29), 10532-7.

48. Casabona, M.G. et al. (2017) Functional analysis of the EsaB component of the *Staphylococcus aureus* Type VII secretion system. Microbiology.

49. Casabona, M.G. et al. (2017) Haem-iron plays a key role in the regulation of the Ess/type VII secretion system of *Staphylococcus aureus* RN6390. Microbiology 163 (12), 1839-1850.

50. Horsburgh, M.J. et al. (2001) In *Staphylococcus aureus*, fur is an interactive regulator with PerR, contributes to virulence, and Is necessary for oxidative stress resistance through positive regulation of catalase and iron homeostasis. J Bacteriol 183 (2), 468-75.

51. Johnson, M. et al. (2011) Fur is required for the activation of virulence gene expression through the induction of the sae regulatory system in *Staphylococcus aureus*. Int J Med Microbiol 301 (1), 44-52.

52. Liang, X. et al. (2005) Global regulation of gene expression by ArlRS, a two-component signal transduction regulatory system of *Staphylococcus aureus*. J Bacteriol 187 (15), 5486-92.

53. Groicher, K.H. et al. (2000) The *Staphylococcus aureus* lrgAB operon modulates murein hydrolase activity and penicillin tolerance. J Bacteriol 182 (7), 1794-801.

54. Patton, T.G. et al. (2006) The role of proton motive force in expression of the *Staphylococcus aureus* cid and lrg operons. Mol Microbiol 59 (5), 1395-404.

55. Sharma-Kuinkel, B.K. et al. (2009) The *Staphylococcus aureus* LytSR two-component regulatory system affects biofilm formation. J Bacteriol 191 (15), 4767-75.

56. Kinkel, T.L. et al. (2013) The *Staphylococcus aureus* SrrAB two-component system promotes resistance to nitrosative stress and hypoxia. MBio 4 (6), e00696-13.

57. Neumann, Y. et al. (2015) The effect of skin fatty acids on *Staphylococcus aureus*. Arch Microbiol 197 (2), 245-67.

58. Desbois, A.P. and Smith, V.J. (2010) Antibacterial free fatty acids: activities, mechanisms of action and biotechnological potential. Appl Microbiol Biotechnol 85 (6), 1629-42.

59. Nguyen, M.T. et al. (2016) Skin-Specific Unsaturated Fatty Acids Boost the *Staphylococcus aureus* Innate Immune Response. Infect Immun 84 (1), 205-15.

60. Arsic, B. et al. (2012) Induction of the staphylococcal proteolytic cascade by antimicrobial fatty acids in community acquired methicillin resistant *Staphylococcus aureus*. PLoS One 7 (9), e45952.

61. Kelsey, J.A. et al. (2006) Fatty acids and monoacylglycerols inhibit growth of *Staphylococcus aureus*. Lipids 41 (10), 951-61.

62. Kohler, T. et al. (2009) Wall teichoic acid protects *Staphylococcus aureus* against antimicrobial fatty acids from human skin. J Bacteriol 191 (13), 4482-4.

63. Moran, J.C. et al. (2017) Comparative Transcriptomics Reveals Discrete Survival Responses of *S. aureus* and *S. epidermidis* to Sapienic Acid. Front Microbiol 8, 33.

64. Alnaseri, H. et al. (2015) Inducible Expression of a Resistance-Nodulation-Division-Type Efflux Pump in *Staphylococcus aureus* Provides Resistance to Linoleic and Arachidonic Acids. J Bacteriol 197 (11), 1893-905.

65. Truong-Bolduc, Q.C. et al. (2014) Native efflux pumps contribute resistance to antimicrobials of skin and the ability of *Staphylococcus aureus* to colonize skin. J Infect Dis 209 (9), 1485-93.

66. Geiger, T. et al. (2012) The stringent response of *Staphylococcus aureus* and its impact on survival after phagocytosis through the induction of intracellular PSMs expression. PLoS Pathog 8 (11), e1003016.

67. Mashruwala, A.A. et al. (2017) Impaired respiration elicits SrrAB-dependent programmed cell lysis and biofilm formation in *Staphylococcus aureus*. Elife 6.

68. Cox, J. et al. (2014) Accurate proteome-wide label-free quantification by delayed normalization and maximal peptide ratio extraction, termed MaxLFQ. Mol Cell Proteomics 13 (9), 2513-26.

69. Ritchie, M.E. et al. (2015) limma powers differential expression analyses for RNA-sequencing and microarray studies. Nucleic Acids Res 43 (7), e47.

70. Schindelin, J. et al. (2012) Fiji: an open-source platform for biological-image analysis. Nat Methods 9 (7), 676-82.

71. Smith, A.F. et al. (2019) Elucidation of glutamine lipid biosynthesis in marine bacteria reveals its importance under phosphorus deplete growth in *Rhodobacteraceae*. ISME J 13 (1), 39-49.

72. Varemo, L. et al. (2013) Enriching the gene set analysis of genome-wide data by incorporating directionality of gene expression and combining statistical hypotheses and methods. Nucleic Acids Res 41 (8), 4378-91.

73. Fey, P.D. et al. (2013) A genetic resource for rapid and comprehensive phenotype screening of nonessential *Staphylococcus aureus* genes. MBio 4 (1), e00537-12.

Figure legends

Figure 1. EsxC contributes to *S. aureus* membrane architecture. Bacteria were grown aerobically to OD_{600} of 1. (*A*) Widefield micrographs of *S. aureus* USA300 JE2 wild-type (WT), its isogenic mutant Δ*esxC*, Δ*esxC* containing the empty pOS1 plasmid, and the complemented strain Δ*esxC* p*esxC* (pOS1-*esxC*) after staining with FM4-64 and DAPI. The composite images were obtained by merging phase contrast and FM4-64 images. The images are representative of 3 independent experiments. (*B*) The FM4-64 fluorescence of bacterial clusters from 9 different fields per strain was quantitated with ImageJ. Data are shown as box-and-whisker plots, where the whiskers extend to the highest and lowest FM4-64 intensities, the median is the vertical bar inside the box, whose ends are the lower and upper quartiles. After a two-tailed t-test, *** $P < 0.001$. (*C*) The membrane fluidity of WT and Δ*esxC* was measured with pyrene decanoic acid staining based assay, and is presented as a percentage of the WT, which was set to 100%. Data presented are means and error bars represent standard deviation (SD) of 6 independent experiments. ** indicates $P < 0.01$ using a Mann-Whitney U test.

Figure 2. Altered surfome in the absence of surface-associated EsxC. (*A*) Immunoblot analysis of membrane (MEMB) or cell wall (CW) fractions of USA300 JE2 wild-type (WT), Δ*essC*, and Δ*esxC* with anti-EsxC sera or anti-PBP2a antibodies (loading control). (*B*) Volcano plot of the quantitative proteomic analysis of surface proteins in Δ*esxC* compared to WT. The relative abundance of each protein (log_2 fold change, X-axis) and its statistical significance (*P* value, Y-axis) are shown in the graph. Proteins decreased by more than half in Δ*esxC* (log_2 fold change < -1 and *P* value < 0.05) are shown in green. (*C*) The ratios of WT, Δ*esxC* or Δ*essC* bacteria that survived a 2h-treatment with 0.1% Triton X-100 were determined using the bacterial CFU at t =

0 (~ 2 × 10^8 CFU/mL). Percentage survival of mutants relative to the WT are shown. Data presented are means of 4 independent experiments and error bars represent SD. * indicates $P < 0.05$ using a Kruskal-Wallis test with Dunn's test relative to WT. (*D*) Representative picture of bacteria before and after a triton-challenge as described in (*C*).

Figure 3. Enhanced *S. aureus* growth inhibition by linoleic acid upon *essC* or *esxC* deletion. (*A*) *S. aureus* USA300 JE2 wild-type (WT) and the *essC* (Δ*essC*) or *esxC* (Δ*esxC*) deletion mutant were grown in TSB or TSB supplemented with 80 μM of either linoleic (LA) or stearic acid (SA). Data shown are the means ± standard error of the mean (SEM). (*B*) After 14h of growth as described in (*A*) Bacteria were serially diluted, and colony counts were determined. Data presented are the means and the error bars represent SD of 3 independent experiments. ** indicates $P < 0.01$ using one-way ANOVA with Dunnett's test relative to WT grown in TSB + LA. (*C*) USA300 JE2 WT with the empty pOS1 plasmid (WT pOS1) and USA300 JE2 *esxC* mutant with either pOS1 (Δ*esxC* pOS1) or pOS1-*esxC* (Δ*esxC* pOS1-*esxC*) were grown in TSB or TSB + 80 μM LA as described in (*A*), plated and counted. Data shown are means and error bars represent SD of 5 independent experiments. ** indicates $P < 0.01$ using one-way ANOVA with Dunnett's test relative to WT pOS1 grown in TSB + LA.

Figure 4. T7SS substrates contribute to resistance to linoleic acid toxicity. (*A*) *S. aureus* USA300 wild-type (WT) and USA300 *esxA* (Δ*esxA*) or *esxB* (Δ*esxB*) deletion mutants were grown in TSB or TSB supplemented with 80 μM linoleic (LA) or stearic acid (SA). (*B*) *S. aureus* Newman WT and Newman *esxA* (Δ*esxA*) or *esxB* (Δ*esxB*) deletion mutants were grown similarly in TSB or TSB + 40 μM LA or SA. (*C*) Newman WT with the empty pOS1 plasmid (WT pOS1) and Newman *esxA* mutant with either pOS1 (Δ*esxA* pOS1) or pOS1-*esxA* (Δ*esxA* p*esxA*) were grown as described in (*B*).

(*D*) Growth curves as described in (*A*) were done with RN6390 wild-type (WT) and RN6390 *essC* (Δ*essC*) or *esxC* (Δ*esxC*) deletion mutants. Data shown as in (*A*), (*B*), (*C*), and (*D*) are representative of at least 3 independent experiments.

Figure 5. T7SS mutants display an increased membrane permeability upon linoleic acid binding. (*A*) Chemical structure of azide functionalised linoleic acid (azide-LA; N^6-diazo-N^2-((9Z,12Z)-octadeca-9,12-dienoyl)lysine, N_3-LA). Highlighted in green is the azido lysine. (*B*) *S. aureus* USA300 JE2 wild-type (WT) and its *essC* (Δ*essC*) or *esxC* (Δ*esxC*) deletion mutants were grown with shaking in TSB to OD_{600} of 1. The bacteria were then stained for 15 min with azide-LA prior to labelling for 1 h with alkyne Alexa Fluor 488. Fluorescence was measured by a fluorimeter, and data presented are percentages of Δ*essC* and Δ*esxC* fluorescence in relation to that of the WT (100%). Data presented are the means and error bars represent SD of 5 independent experiments. (*C*) Micrographs of bacteria grown in TSB and treated as described in (*B*) and additionally stained with propidium iodide (PI). (*D*) ImageJ was used to quantitate PI fluorescence of bacterial clusters from 12 different fields per strain. Each box-and-whisker plot depicts the minimal and maximal PI intensities, and the median is the vertical bar inside the box, which is delimitated by the lower and upper quartiles. ** indicates $P < 0.01$ using one-way ANOVA with Dunnett's test.

Fig. 6. T7SS mutants are less able to incorporate LA into their phospholipids. Representative HPLC chromatograms of native phosphatidylglycerol (PG) species of *S. aureus* USA300 JE2 WT (*A*) or Δ*esxC* (*B*) grown in TSB (top panel) or in TSB supplemented with LA (bottom panel), in negative ionisation mode. (*C*-*D*) Relative quantification of the indicated PG species containing an unsaturated fatty acid in WT, Δ*essC* and Δ*esxC*. C18:2-containing PG species (*C*) and total unsaturated exogenous PG species (*D*) are presented as ratios of total PG species. Data shown are the means

and error bars represent SD of 3 independent experiments. * indicates $P < 0.05$ using one-way ANOVA with Dunnett's test.

Fig. 7. Quantitative proteomics unveils the changed cellular content of the T7SS mutants and its impact on bacterial response to LA. *S. aureus* USA300 JE2 wild-type (WT) and USA300 JE2 mutants (Δ*essC* and Δ*esxC*) were grown in TSB or TSB supplemented with LA. (*A*) Venn diagram showing the number of proteins with altered abundance compared to USA300 JE2 wild-type (WT) specific to Δ*essC* (23) or Δ*esxC* (10), and common to Δ*essC* and Δ*esxC* (14). (*B*) The fourteen proteins that are similarly changed in both *essC* and *esxC* mutants are highlighted on a volcano plot. (*C*) Volcano plot showing the extensive change in the LA-treated WT compared to WT. (*D*) Venn diagram displaying the numbers of proteins with altered relative abundance upon LA challenge of WT (LA.WT), Δ*essC* (LA.dEssC) or Δ*esxC* (LA.dEsxC) compared to the respective untreated samples. (*E*) and (*F*) Heatmaps depicting the *P* values of enriched (*E*) or diminished (*F*) molecular functions following a gene set analysis based on GO (gene ontology) annotations. Molecular functions that are changed in at least one strain ($P < 0.05$) following growth in presence of LA are shown. The shades of blue (*E*) or red (*F*) correspond to $-\log_{10}$ (*P* value).

Figure S1. USA300 JE2 WT and Δ*esxC* strains display similar growth rates. WT and Δ*esxC* were grown in TSB, and OD_{600} monitored with a Novaspec® Pro spectrophotometer. Data shown are means of three independent experiments, and the error bars indicate the standard errors of the mean.

Figure S2. USA300 JE2 WT and T7SS mutants display similar lipids. Representative HPLC chromatograms of the indicated bacteria grown in TSB (*A*) or in

TSB supplemented with LA (*B*), in negative ionisation mode. Phosphatidylglycerol (PG) is highlighted.

Figure S3. Δ*essC* can incorporate LA into its phosphatidylglycerol (PG) species. Representative HPLC chromatograms of native PG species of Δ*essC* grown in TSB (top panel) or in TSB supplemented with LA (bottom panel), in negative ionisation mode.

Figure S4. LA (C18:2) is elongated and incorporated into *S. aureus* phosphatidylglycerol (PG) species. Representative mass spectrometry fragmentation spectra for PG species containing unsaturated fatty acids, in negative ionisation mode. (*A*) PG species with mass 731 m/z, containing C18:2 fatty acid (279 m/z). (*B*) PG species 759 m/z, containing C20:2 fatty acid (307 m/z) (*C*) PG species 787 m/z, containing C22:2 fatty acid (335 m/z).

Figure S5. PG species containing elongated LA are present in USA300 JE2 WT and T7SS mutants. Relative quantification of the indicated PG species containing an unsaturated fatty acid in WT, Δ*essC* and Δ*esxC*. C20:2- (*A*) and C22:2-containing PG species (*B*) are presented as ratios of total PG species. Data shown are the means and error bars represent SD of 3 independent experiments.

Figure S6. Principal component analysis (PCA) of the *S. aureus* cellular proteomic profiles. PCA were performed on all the identified proteins of USA300 JE2 WT and T7SS mutants grown in TSB (untreated) or TSB + LA (LA-treated). Each dot represents a biological replicate.

Figure S7. ^{1}H NMR spectra of NHS-LA (*A*) and azide-LA (*B*) in $CDCl_3$. Both spectra were recorded on a Bruker Advance 300 spectrometer (300 MHz) at 27 °C.

The letters indicate the chemical shift δ (in parts per million, ppm) of the protons in each molecule.

Table 1. Surface proteins significantly changed in Δ*esxC* mutant relative to WT USA300 JE2.

Uniprot ID	log_2 FC	*P* Value	Description	Localization
A0A0H2XJV9	0.7	0.0069	Surface protein G	Cell wall
A0A0H2XHF6	0.7	0.0383	Secretory antigen SsaA	Extracellular
Q2FE03	0.6	0.0350	Fibronectin-binding protein A FnbA	Cell wall
Q2FG28	-1.7	0.0217	Putative universal stress protein	Cytoplasm
A0A0H2XFG6	-1.4	0.0110	Uncharacterized secreted protein	Extracellular
Q2FFJ6	-1.4	0.0326	Amidotransferase subunit B GatB	Cytoplasm
A0A0H2XFP1	-1.2	0.0281	ESAT-6 secretion accessory factor EsaA	Membrane
A0A0H2XGD7	-1.1	0.0002	ATP-dependent 6-phosphofructokinase PfkA	Cytoplasm
Q2FI15	-1.1	0.0003	Bifunctional protein FolD	Cytoplasm
Q2FEV0	-1.1	0.0046	Alkaline shock protein 23	Cytoplasm
A0A0H2XIJ1	-1.1	0.0322	Enoyl-[acyl-carrier-protein] reductase [NADPH] FabI	Cytoplasm
Q2FJM6	-1.0	0.0345	Inosine-5-monophosphate dehydrogenase	Cytoplasm
A0A0H2XDE4	-0.9	0.0130	Transcriptional regulator MgrA	Cytoplasm
Q2FJM5	-0.9	0.0140	GMP synthase [glutamine-hydrolyzing]	Cytoplasm
Q2FFV6	-0.9	0.0182	S-adenosylmethionine synthase MetK	Cytoplasm
A0A0H2XGP3	-0.8	0.0339	UDP-N-acetylglucosamine 1-carboxyvinyltransferase MurA	Cytoplasm
Q2FJA0	-0.8	0.0421	50S ribosomal protein L7/L12	Cytoplasm
A0A0H2XH82	-0.7	0.0202	Putative lipoprotein	Membrane
Q2FJE0	-0.7	0.0378	50S ribosomal protein L25	Cytoplasm
A0A0H2XFW2	-0.6	0.0035	Universal stress family protein	Cytoplasm
Q2FG40	-0.5	0.0373	Pyruvate kinase	Cytoplasm
Q2FHV1	-0.5	0.0423	Iron-regulated surface determinant protein A IsdA	Cell wall
Q2FID4	-0.4	0.0421	NADH dehydrogenase-like protein	Cytoplasm

Table 2. Proteins with changed abundance in Δ*essC* and Δ*esxC* mutants relative to the WT USA300 JE2

		Δ*essC*/WT		Δ*esxC*/WT		
Functions	**Uniprot ID**	**Log_2 FC**	**Adjusted *P* value**	**Log_2 FC**	**Adjusted *P* value**	**Description**
Signal transduction systems	Q2FK09	-3.0	4.90E-13	-3.1	4.90E-13	Sensory transduction protein LytR
	Q2FH23	-2.9	0.002527	-2.1	0.026184	Response regulator ArlR
Membrane proteins	A0A0H2XF42	3.0	1.75E-10	0	1	Cytochrome D ubiquinol oxidase, subunit I
	A0A0H2XDZ5	1.7	1.68E-05	0	1	Uncharacterized membrane protein
	A0A0H2XFJ8	2.0	0.001077	0.5	0.883953	Uracil permease
	A0A0H2XGW7	2.7	0.005757	2.5	0.010784	Putative lipoprotein
	A0A0H2XIA9	1.0	0.006115	0	1	Protein translocase subunit SecY
	Q2FIN2	1.6	0.029451	0.5	0.970614	Prolipoprotein diacylglyceryl transferase LGT
	A0A0H2XKD9	2.0	0.038093	1.8	0.070347	Staphylococcal respiratory response protein SrrB
	A0A0H2XFE1	3.4	0.039814	1.1	0.970614	Peptidase
	A0A0H2XJV8	2.0	0.04444	1.5	0.231285	Cyclic-di-AMP phosphodiesterase
	A0A0H2XGF4	3.0	0.044681	0.9	0.986458	Sodium:dicarboxylate symporter family protein
	A0A0H2XHV2	2.5	0.049168	2.4	0.070182	Glycine betaine transporter OpuD
Stress response	A0A0H2XKH6	2.2	5.80E-05	2.5	1.07E-05	Universal stress protein family
	A0A0H2XIZ0	0.0	1	-3.4	1. 06E-10	OsmC/Ohr family protein
DNA repair	Q2FHE2	-2.3	1.79E-08	-2.3	1.19E-08	DNA mismatch repair protein MutL
	A0A0H2XI63	-2.0	0.004036	-2.0	0.004036	DNA repair protein RadA
	A0A0H2XHT1	-0.3	0.708343	-1.9	0.008379	Formamidopyrimidine-DNA glycosylase MutM
Oxidation-reduction process	A0A0H2XJ90	1.1	0.038093	1.0	0.088334	D-isomer specific 2-hydroxyacid dehydrogenase family protein
	A0A0H2XHE0	2.4	0.039099	-0.1	1	Thiol-disulphide oxidoreductase, DCC family protein
	A0A0H2XGR9	0.0	1	1.4	8.89E-08	Oxidoreductase, Gfo/Idh/MocA family
	A0A0H2XK08	1.0	0.406975	2.9	0.00791	Oxidoreductase, short chain dehydrogenase/reductase family
	A0A0H2XFZ3	-0.8	0.404225	2.1	0.016405	Nitroreductase family protein
Hydrolases	A0A0H2XE49	2.9	1.07E-06	2.9	5.99E-07	Amidohydrolase
	Q2FES9	-2.7	0.003385	-0.3	1	Uncharacterized hydrolase
	A0A0H2XFF2	-0.8	0.016697	-0.5	0.157809	Peptidase, U32 family
	A0A0H2XJH8	0.0	1	2.8	1.06E-10	Peptidase M20 domain-containing protein 2
	A0A0H2XJ54	0.0	1	2.0	0.000949	Hydrolase (HAD superfamily)
	Q2FEG2	-0.2	0.854748	-2.9	0.004615	Formimidoylglutamase
Metabolism	A0A0H2XGU2	-1.6	4.99E-06	-0.1	1	Pseudouridine synthase
	A0A0H2XK15	2.8	0.004424	0.9	0.777138	1-phosphatidylinositol phosphodiesterase
	Q2FEK2	-1.6	0.038093	-0.3	1	Urease accessory protein UreE
	Q2FI05	1.1	0.038093	0.0	1	Bifunctional purine biosynthesis protein PurH
	Q2FIL2	2.9	0.038093	0.8	0.970614	SsrA-binding protein
	A0A0H2XII6	1.8	0.038093	1.5	0.088334	Orn/Lys/Arg decarboxylase
	A0A0H2XJR8	-0.9	0.04444	-0.5	0.61246	RNA methyltransferase, RsmD family
	A0A0H2XKG7	0.0	1	1.4	8.18E-08	Aspartokinase
Cell wall composition	A0A0H2XJQ4	-4.0	4.92E-11	-4.0	3.28E-11	Acetyltransferase, GNAT family
	A0A0H2XKG3	-2.3	0.001238	-1.7	0.016405	Fibronectin binding protein B
	A0A0H2XJC8	-2.3	0.009779	-3.0	0.000819	Phi77 ORF017-like protein (Toxin MazF)
	Q2FE03	0.0	1	2.6	1.18E-12	Fibronectin-binding protein A
Nucleotide binding	A0A0H2XHY5	-2.3	8.58E-06	-2.3	6.01E-06	ATP-grasp domain protein
	A0A0H2XFA5	3.3	0.014259	3.5	0.008379	Putative GTP-binding YqeH protein
Uncharacterised proteins	A0A0H2XGJ8	2.2	0.000372	2.4	9.41E-05	Uncharacterized protein
	A0A0H2XE09	2.1	0.008231	1.9	0.016405	Ybbr-like uncharacterized protein
	Q2FFI4	3.4	0.020136	0.9	0.970614	UPF0316 membrane protein
	A0A0H2XG24	1.1	0.022345	0.8	0.088334	Uncharacterized protein

Table 3. Strains and plasmids used in this study.

Strain or plasmid	Description	Source or reference
Staphylococcus aureus		
USA300 LAC	Community-acquired MRSA (CA-MRSA)	Olaf Schneewind
LAC Δ*esxA*	*S. aureus* USA300 LAC defective for EsxA	[21]
LAC Δ*esxB*	*S. aureus* USA300 LAC defective for EsxB	[21]
USA300 LAC JE2	Plasmid-cured USA300 LAC	BEI Resources (NARSA) [73]
JE2 Δ*esxC*	*S. aureus* USA300 LAC JE2 defective for EsxC	This study
JE2 Δ*essC*	*S. aureus* USA300 LAC JE2 defective for EssC	This study
Newman	Methicillin-sensitive *Staphylococcus aureus*	Olaf Schneewind
Newman Δ*esxA*	*S. aureus* Newman defective for EsxA	[21]
Newman Δ*esxB*	*S. aureus* Newman defective for EsxB	[21]
RN6390	NCTC8325 derivative, Δ*rbsU*, Δ*tcaR*, cured of φ11, φ12, and φ13	Tracy Palmer [14]
RN6390 Δ*esxC*	*S. aureus* RN6390 defective for EsxC	Tracy Palmer [14]
RN6390 Δ*essC*	*S. aureus* RN6390 defective for EssC	Tracy Palmer [14]
RN4220	*S. aureus* restriction negative, cloning tool	BEI Resources (NARSA)
Plasmids		
pKORI	Temperature-sensitive allelic exchange vector	Olaf Schneewind [33]
pKORIΔ*essC*	pKORI used to generate *essC* mutant	This study
pKORIΔ*esxC*	pKORI used to generate *esxC* mutant	This study
pOS1	Insertless vector for genetic complementation	Olaf Schneewind
pOS1CK	pOS1 with P1 constitutive promoter of *sarA*	[21]
pOS1-*esxA*	*esxA* complementation vector	[21]
pOS1-*esxC*	*esxC* complementation vector	This study

Table 4. Primers used in this study.

Primer	Sequence (5' – 3')	Product
AttB1-*esxC* Up-Fwrd	GGGGACAAGTTTGTACAAAAAAGCAGGCTGAGCTAACGCTATGAAAACACC	AttB1-Δ*esxC*-AttB2
esxC-up-Rev-soeing	ACCCATATCTTCACCTCAATAAACATACCTCCCTCCTATTT	
esxC-down-Fwd	TATTGAGGTGAAGATATGGGTGG	
esxC-down-Rev-attB2	GGGGACCACTTTGTACAAGAAAGCTGGGTCGTCATTACTCCTCTGCTTTA	
AttB1-*essC*-up-fwd	GGGGACAAGTTTGTACAAAAAAGCAGGCTGCTACACATTTGTGTTGGCACC	AttB1-Δ*essC*-AttB2
*ess*C-upstream-rev	TGTCTTTGCCTCAGTCCTATAC	
essC-dpwn-soeing-fwd	GTATAGGACTGAGGCAAAGACACAATGAATTAAATAGGAGGGAGG	
esxC-down-Rev-attB2	GGGGACCACTTTGTACAAGAAAGCTGGGTCGTCATTACTCCTCTGCTTTA	
esxC-RBS-PstI-fwd	GCGCTGCAGTTGAGAGGAGAGAAAATGAATTTTAATGATATTGAAAC	RBS-*esxC*
esxC-SmaI-rev	GCGGCGCCCGGGTTAATTCATTGCTTTATTAAA	

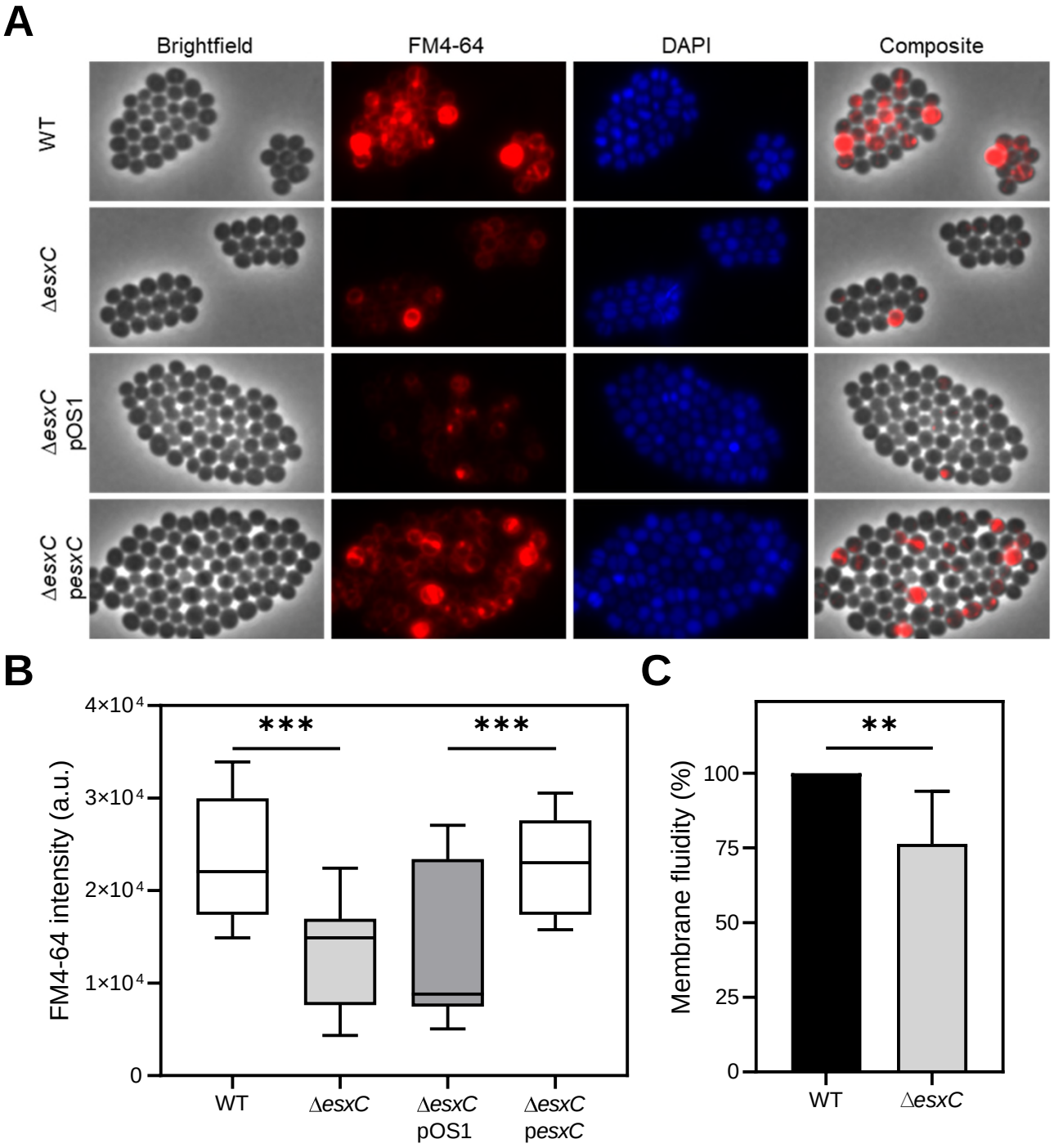
A
Brightfield
FM4-64
DAPI
Composite
WT
ΔesxC
ΔesxC pOS1
ΔesxC pesxC
B
FM4-64 intensity (a.u.)
4×10⁴
3×10⁴
2×10⁴
1×10⁴
0
***
***
WT
ΔesxC
ΔesxC pOS1
ΔesxC pesxC
C
Membrane fluidity (%)
100
75
50
25
0
**
WT
ΔesxC

Fig. 1

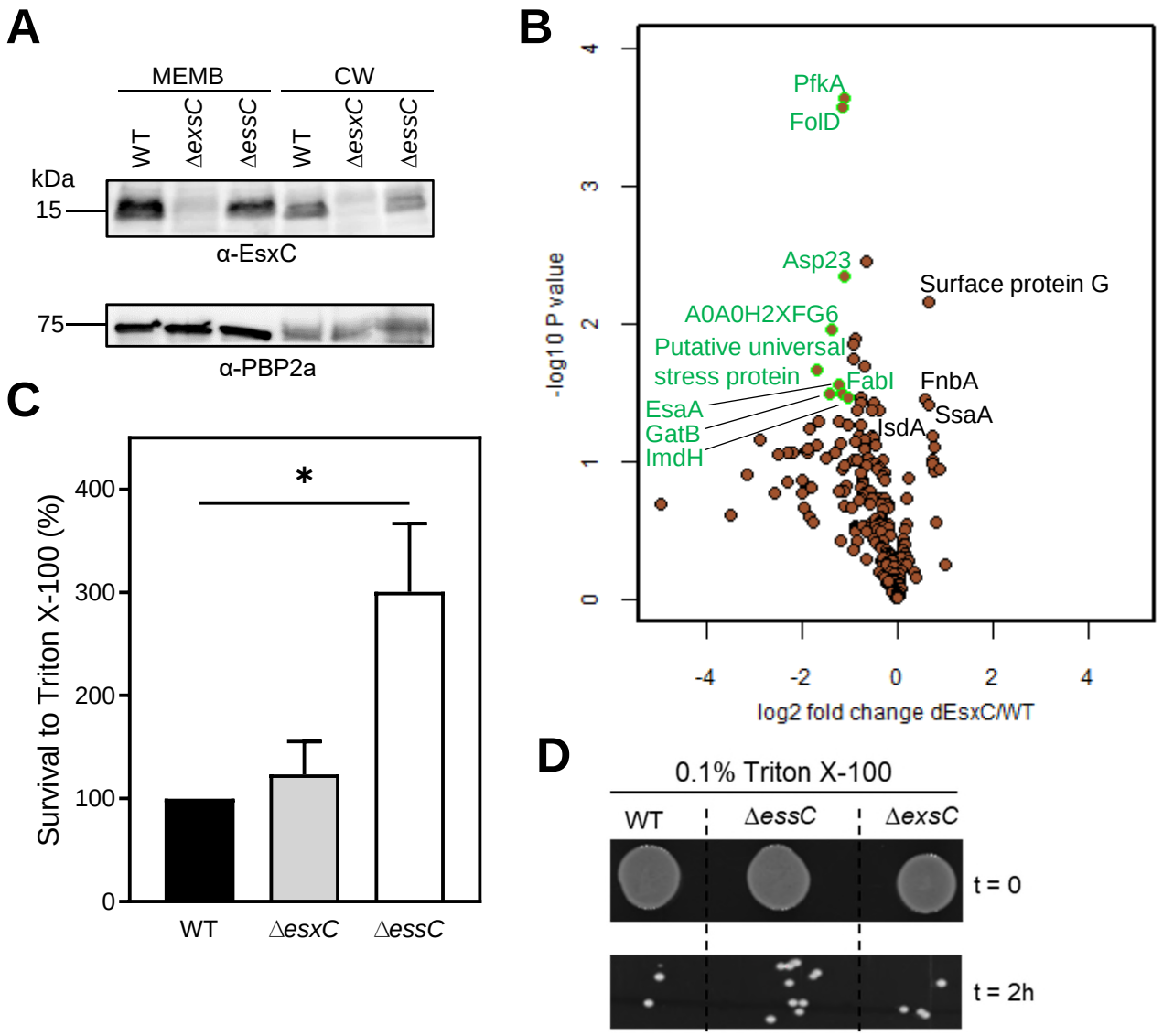
A
MEMB
CW
WT
ΔexsC
ΔessC
WT
ΔexsC
ΔessC
kDa
15
α-EsxC
75
α-PBP2a
B
PfkA
FolD
Asp23
Surface protein G
A0A0H2XFG6
Putative universal
stress protein
FabI
FnbA
SsaA
EsaA
GatB
ImdH
IsdA
-log10 P value
log2 fold change dEsxC/WT
C
Survival to Triton X-100 (%)
*
WT
ΔesxC
ΔessC
D
0.1% Triton X-100
WT
ΔessC
ΔexsC
t = 0
t = 2h

Fig. 2

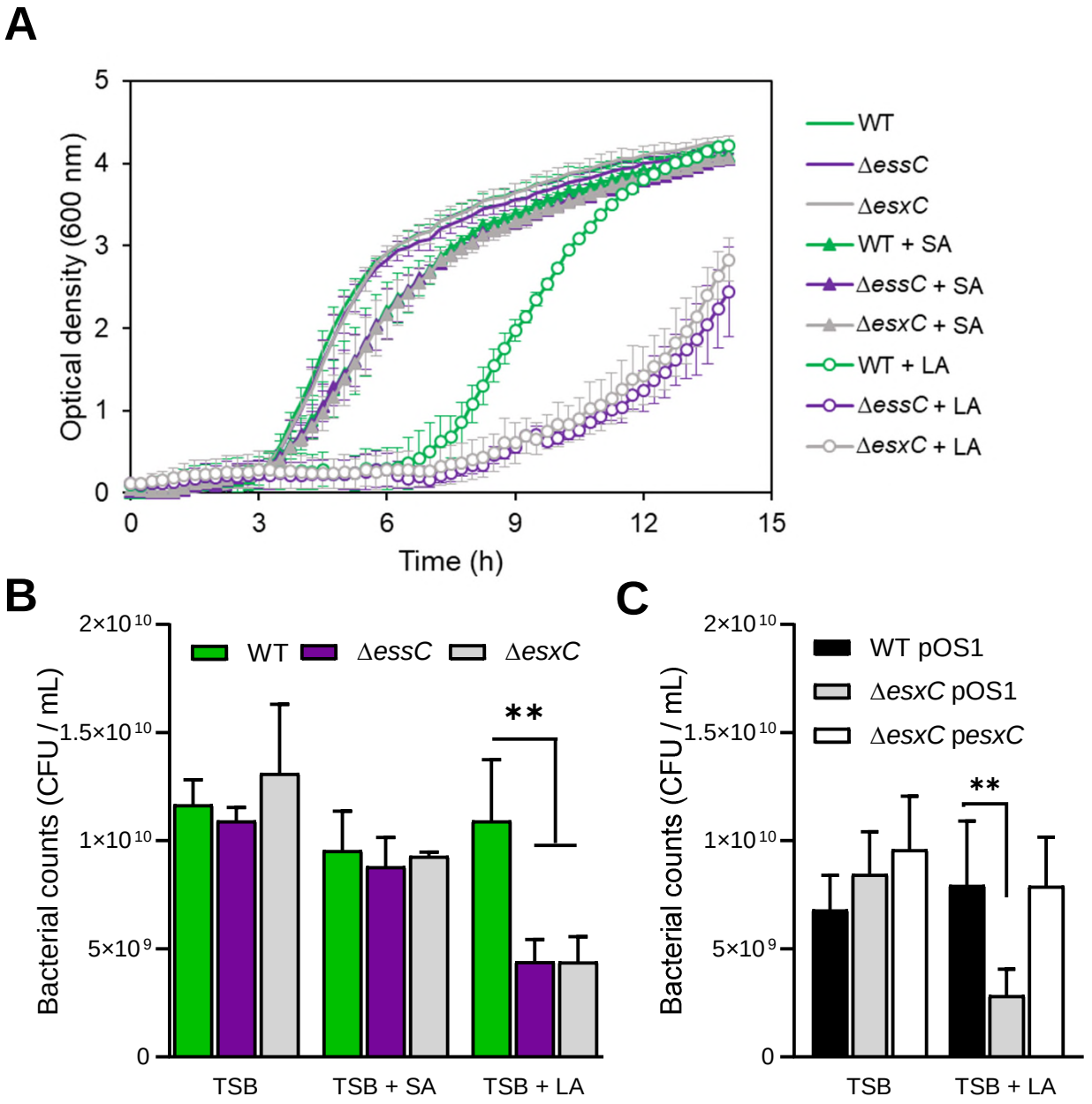
A
Optical density (600 nm)
Time (h)
WT
ΔessC
ΔesxC
WT + SA
ΔessC + SA
ΔesxC + SA
WT + LA
ΔessC + LA
ΔesxC + LA
B
Bacterial counts (CFU / mL)
WT
ΔessC
ΔesxC
**
TSB
TSB + SA
TSB + LA
C
Bacterial counts (CFU / mL)
WT pOS1
ΔesxC pOS1
ΔesxC pesxC
**
TSB
TSB + LA

Fig. 3

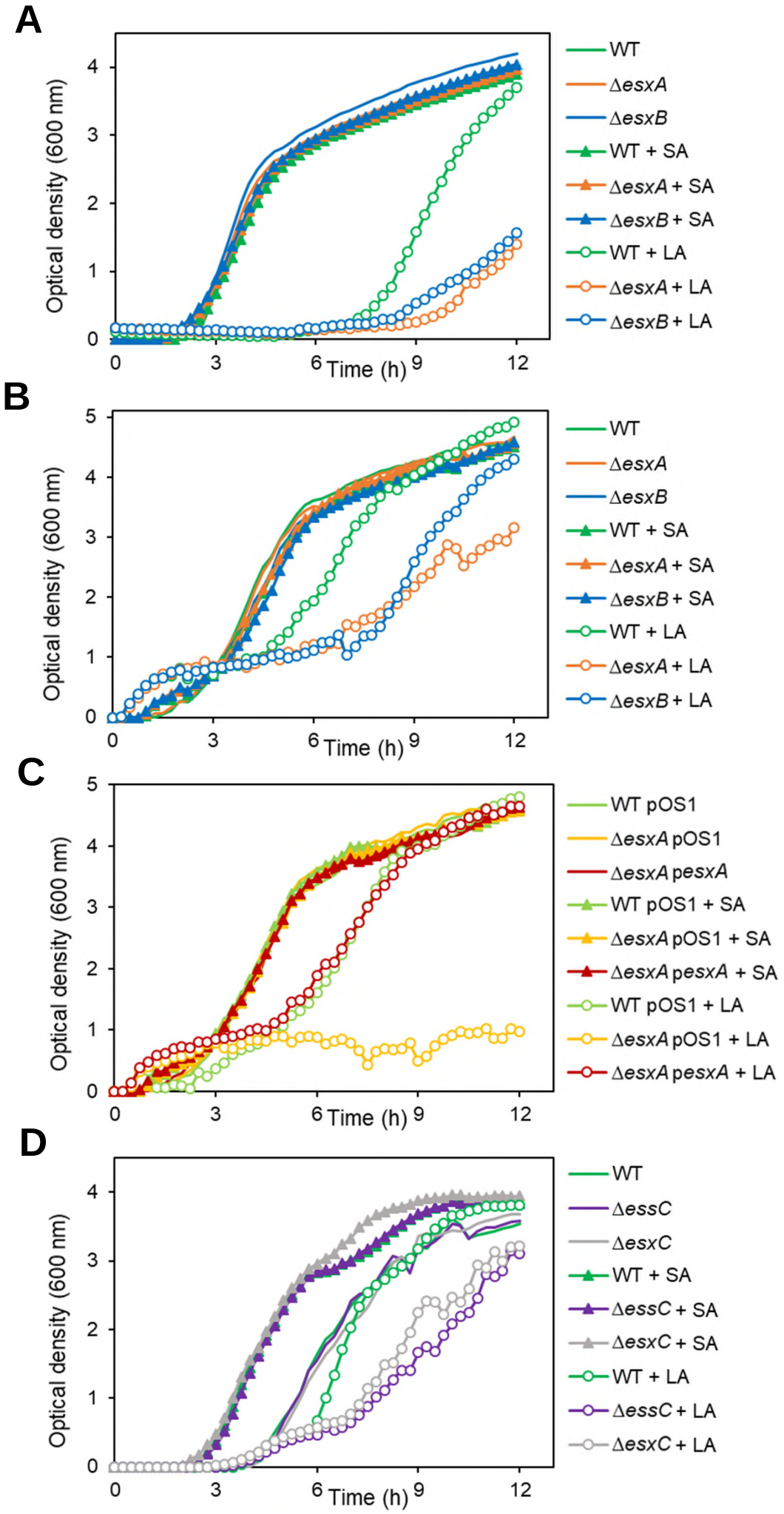
A
Optical density (600 nm)
Time (h)
WT
ΔesxA
ΔesxB
WT + SA
ΔesxA + SA
ΔesxB + SA
WT + LA
ΔesxA + LA
ΔesxB + LA
B
Optical density (600 nm)
Time (h)
WT
ΔesxA
ΔesxB
WT + SA
ΔesxA + SA
ΔesxB + SA
WT + LA
ΔesxA + LA
ΔesxB + LA
C
Optical density (600 nm)
Time (h)
WT pOS1
ΔesxA pOS1
ΔesxA pesxA
WT pOS1 + SA
ΔesxA pOS1 + SA
ΔesxA pesxA + SA
WT pOS1 + LA
ΔesxA pOS1 + LA
ΔesxA pesxA + LA
D
Optical density (600 nm)
Time (h)
WT
ΔessC
ΔesxC
WT + SA
ΔessC + SA
ΔesxC + SA
WT + LA
ΔessC + LA
ΔesxC + LA

Fig. 4

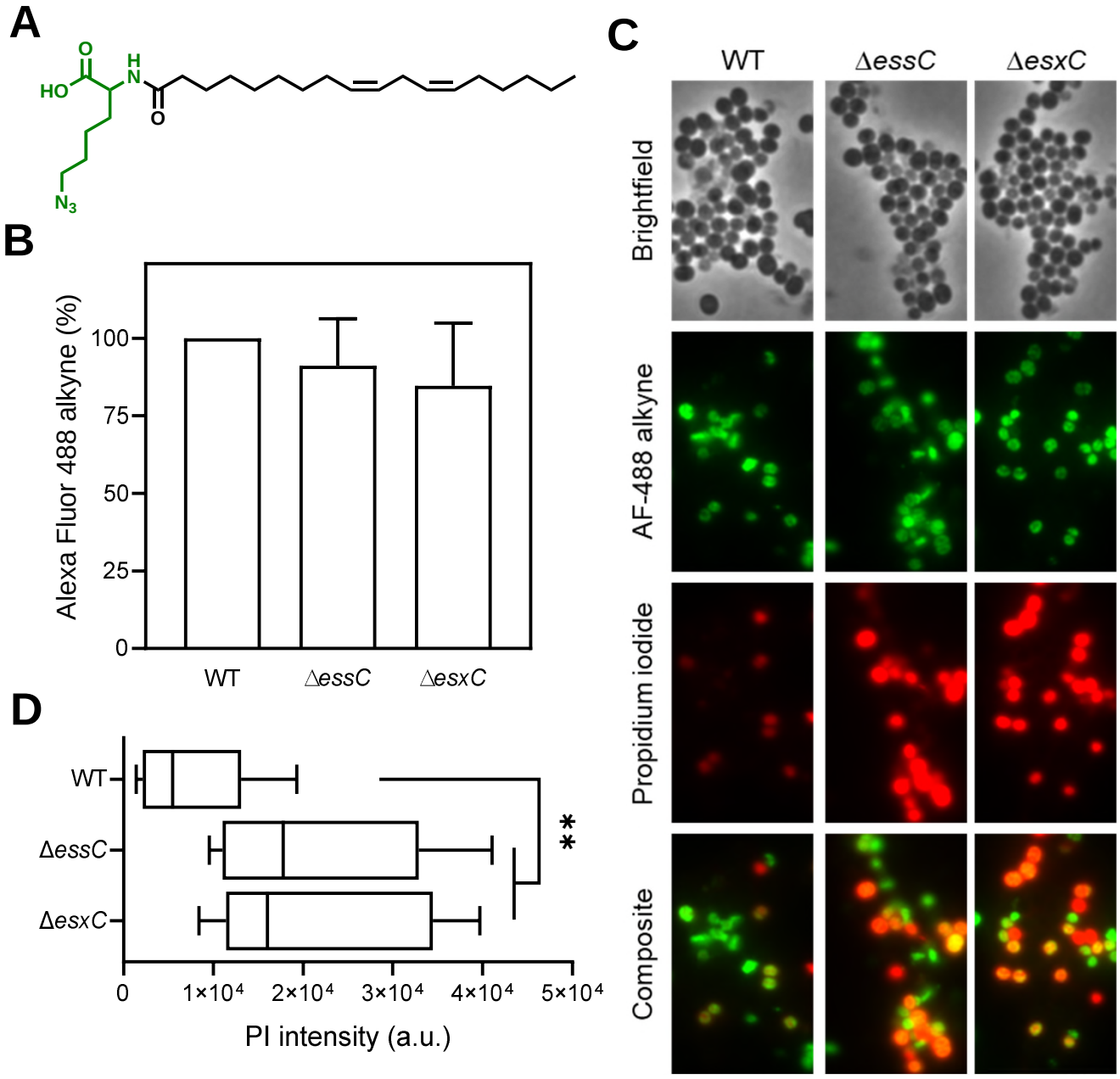
A
HO
O
H
N
O
N3
B
Alexa Fluor 488 alkyne (%)
100
75
50
25
0
WT
ΔessC
ΔesxC
C
WT
ΔessC
ΔesxC
Brightfield
AF-488 alkyne
Propidium iodide
Composite
D
WT
ΔessC
ΔesxC
**
0
1×10⁴
2×10⁴
3×10⁴
4×10⁴
5×10⁴
PI intensity (a.u.)

Fig. 5

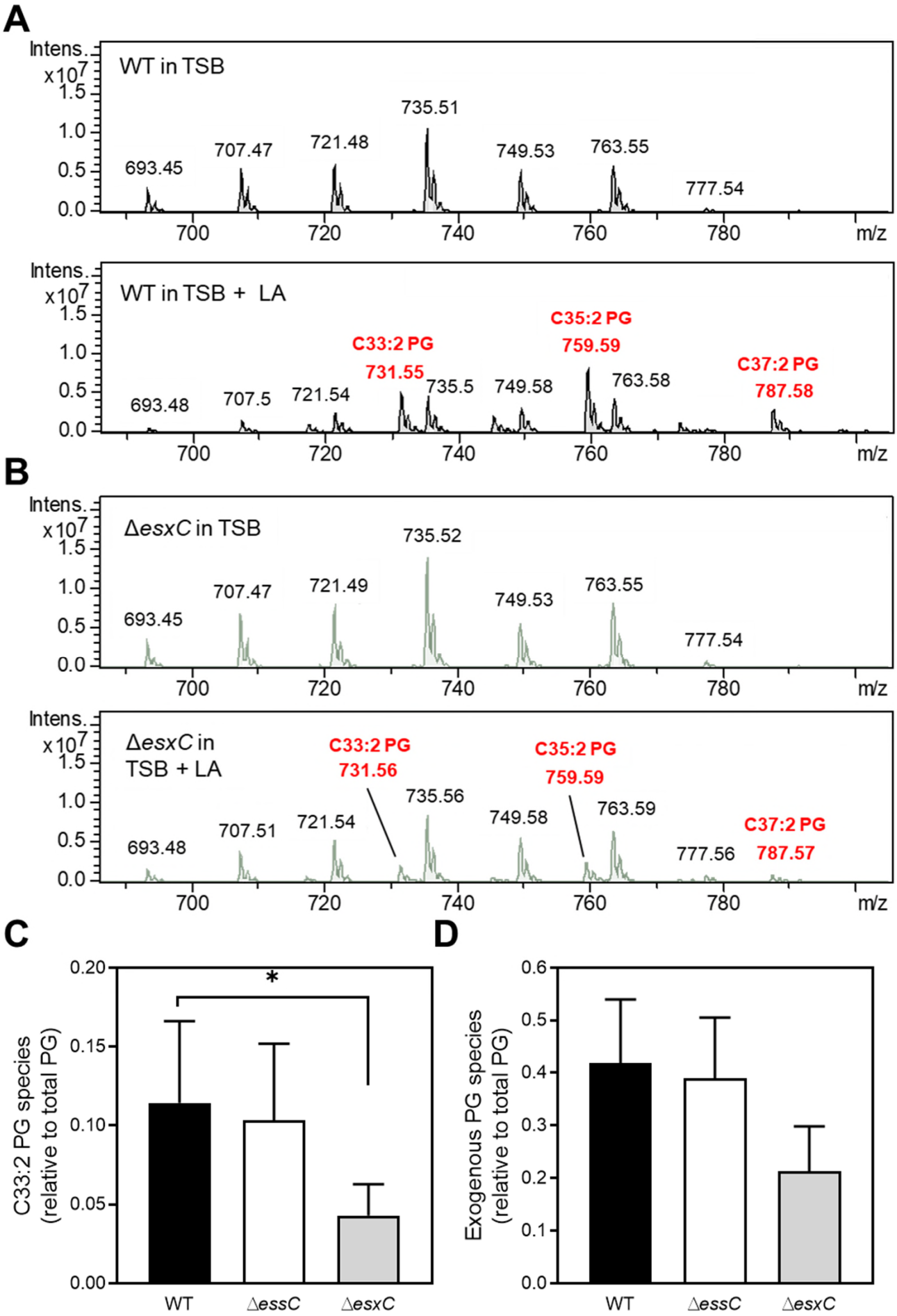
A
Intens.
x10^7
WT in TSB
735.51
707.47
721.48
749.53
763.55
693.45
777.54
m/z
WT in TSB + LA
C35:2 PG
759.59
C33:2 PG
731.55
C37:2 PG
787.58
693.48
707.5
721.54
735.5
749.58
763.58
B
ΔesxC in TSB
735.52
707.47
721.49
749.53
763.55
693.45
777.54
ΔesxC in
TSB + LA
C33:2 PG
731.56
C35:2 PG
759.59
735.56
749.58
763.59
707.51
721.54
693.48
777.56
C37:2 PG
787.57
C
C33:2 PG species
(relative to total PG)
*
WT
ΔessC
ΔesxC
D
Exogenous PG species
(relative to total PG)
WT
ΔessC
ΔesxC

Fig. 6

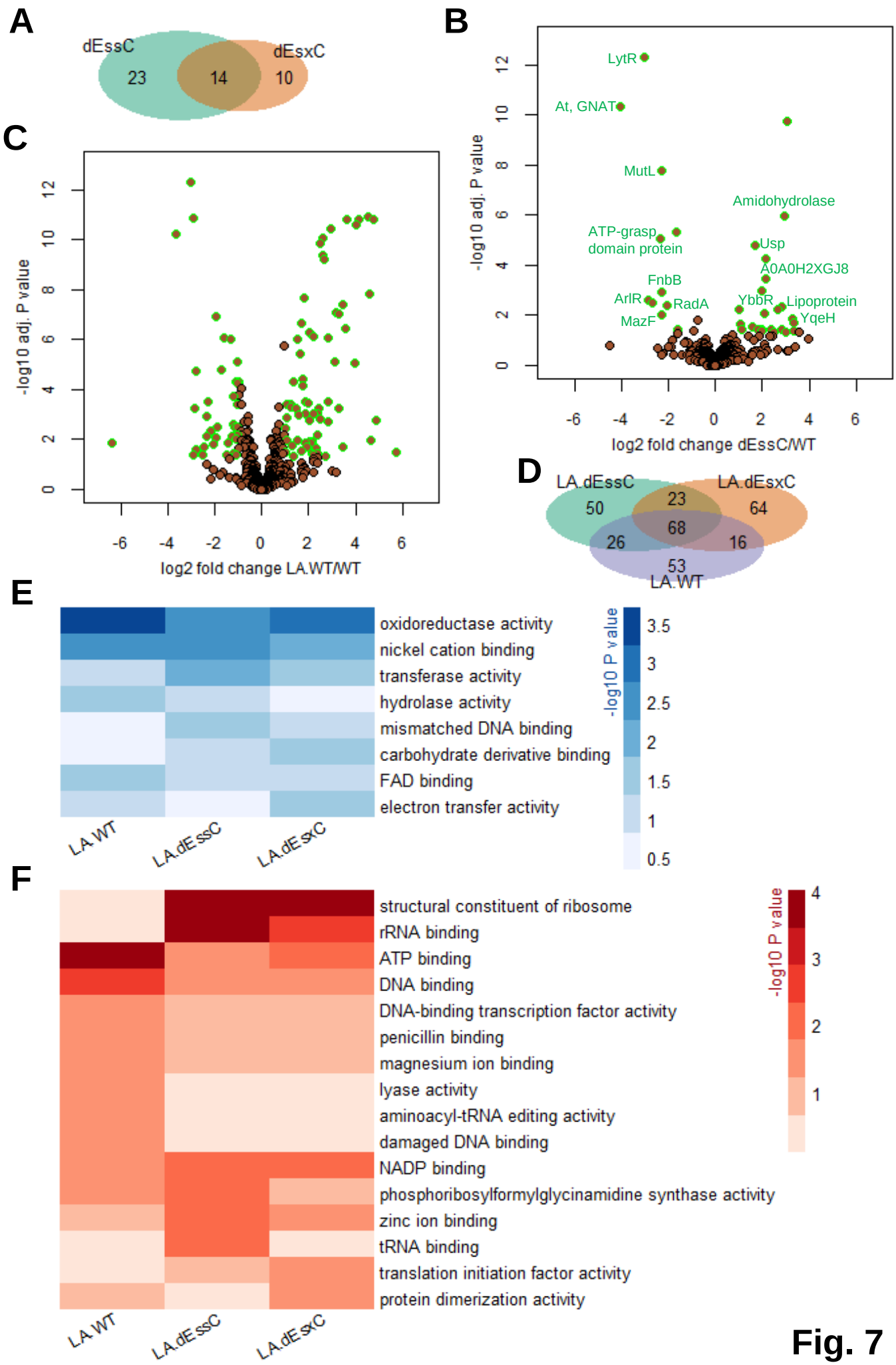
A
dEssC
dEsxC
23
14
10
B
LytR
At, GNAT
MutL
Amidohydrolase
ATP-grasp domain protein
Usp
A0A0H2XGJ8
FnbB
ArlR
RadA
YbbR
Lipoprotein
YqeH
MazF
-log10 adj. P value
log2 fold change dEssC/WT
C
-log10 adj. P value
log2 fold change LA.WT/WT
D
LA.dEssC
LA.dEsxC
LA.WT
50
23
64
68
26
16
53
E
oxidoreductase activity
nickel cation binding
transferase activity
hydrolase activity
mismatched DNA binding
carbohydrate derivative binding
FAD binding
electron transfer activity
LA.WT
LA.dEssC
LA.dEsxC
-log10 P value
F
structural constituent of ribosome
rRNA binding
ATP binding
DNA binding
DNA-binding transcription factor activity
penicillin binding
magnesium ion binding
lyase activity
aminoacyl-tRNA editing activity
damaged DNA binding
NADP binding
phosphoribosylformylglycinamidine synthase activity
zinc ion binding
tRNA binding
translation initiation factor activity
protein dimerization activity
LA.WT
LA.dEssC
LA.dEsxC
-log10 P value

Fig. 7

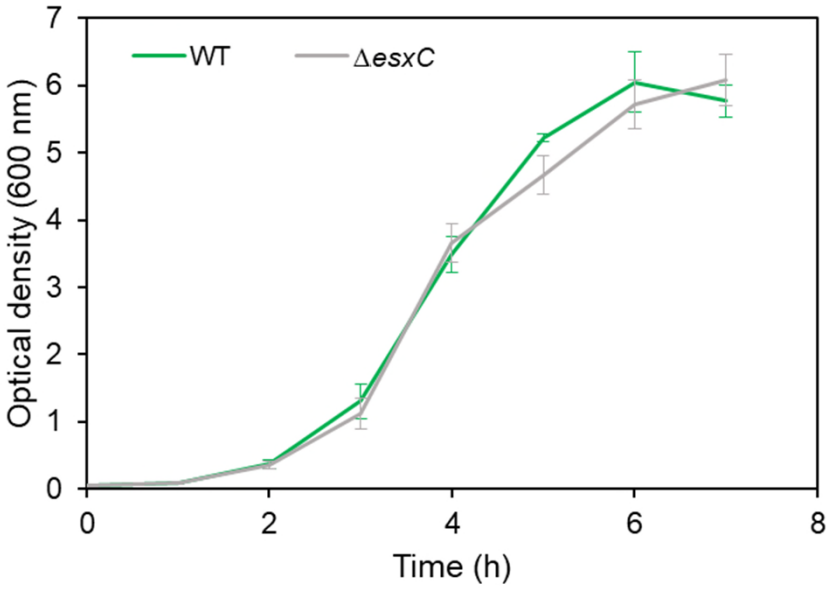

Fig. S1

A

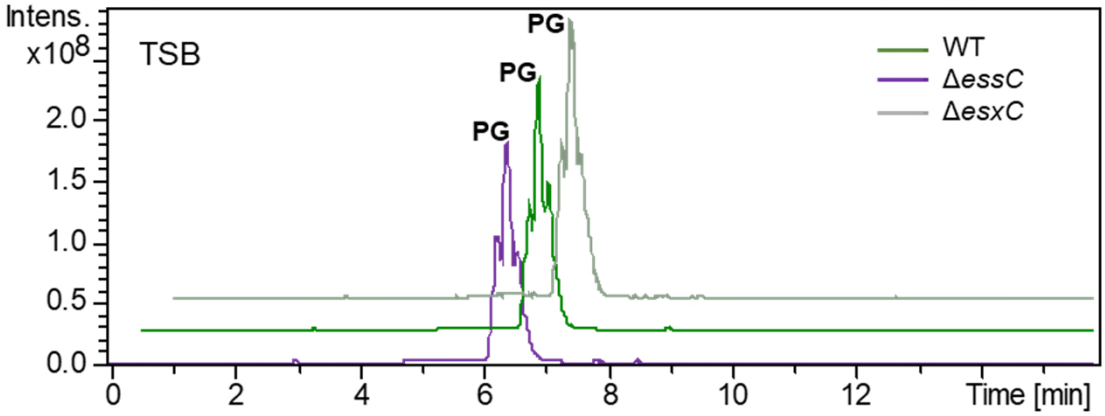
Intens.
x10^8
TSB
PG
PG
PG
WT
ΔessC
ΔesxC
2.0
1.5
1.0
0.5
0.0
0
2
4
6
8
10
12
Time [min]

B

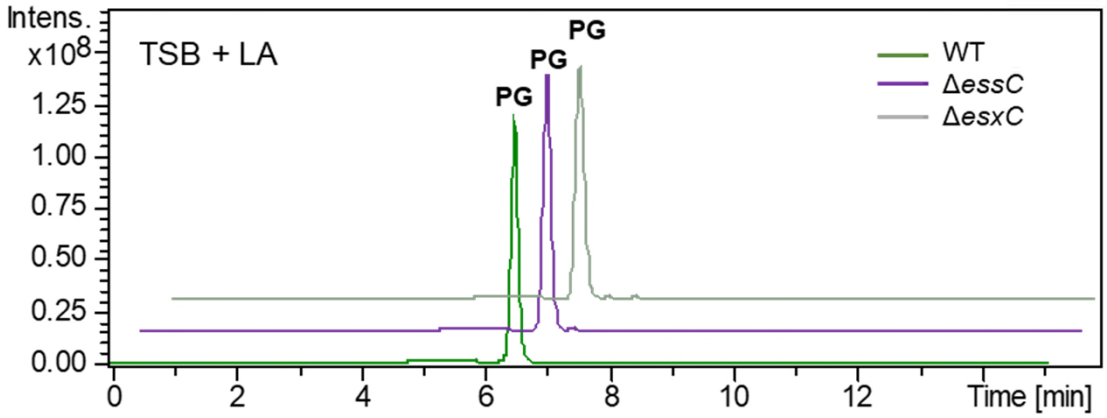
Intens.
x10^8
TSB + LA
PG
PG
PG
WT
ΔessC
ΔesxC
1.25
1.00
0.75
0.50
0.25
0.00
0
2
4
6
8
10
12
Time [min]

Fig. S2

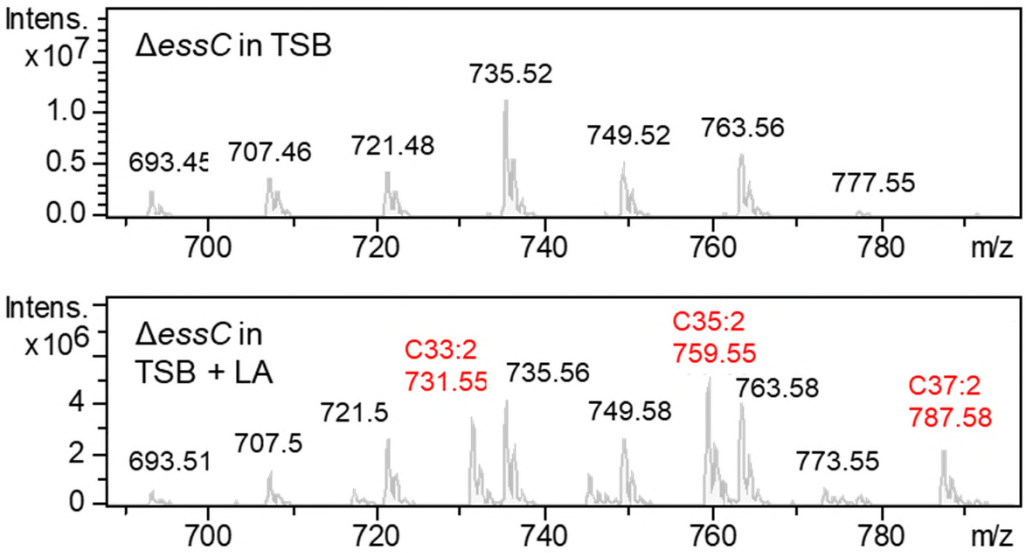
Intens.
x10^7
ΔessC in TSB
735.52
1.0
0.5
0.0
693.45
707.46
721.48
749.52
763.56
777.55
700
720
740
760
780
m/z
Intens.
x10^6
ΔessC in
TSB + LA
C33:2
731.55
735.56
C35:2
759.55
763.58
C37:2
787.58
4
2
0
721.5
749.58
693.51
707.5
773.55
700
720
740
760
780
m/z

Fig. S3

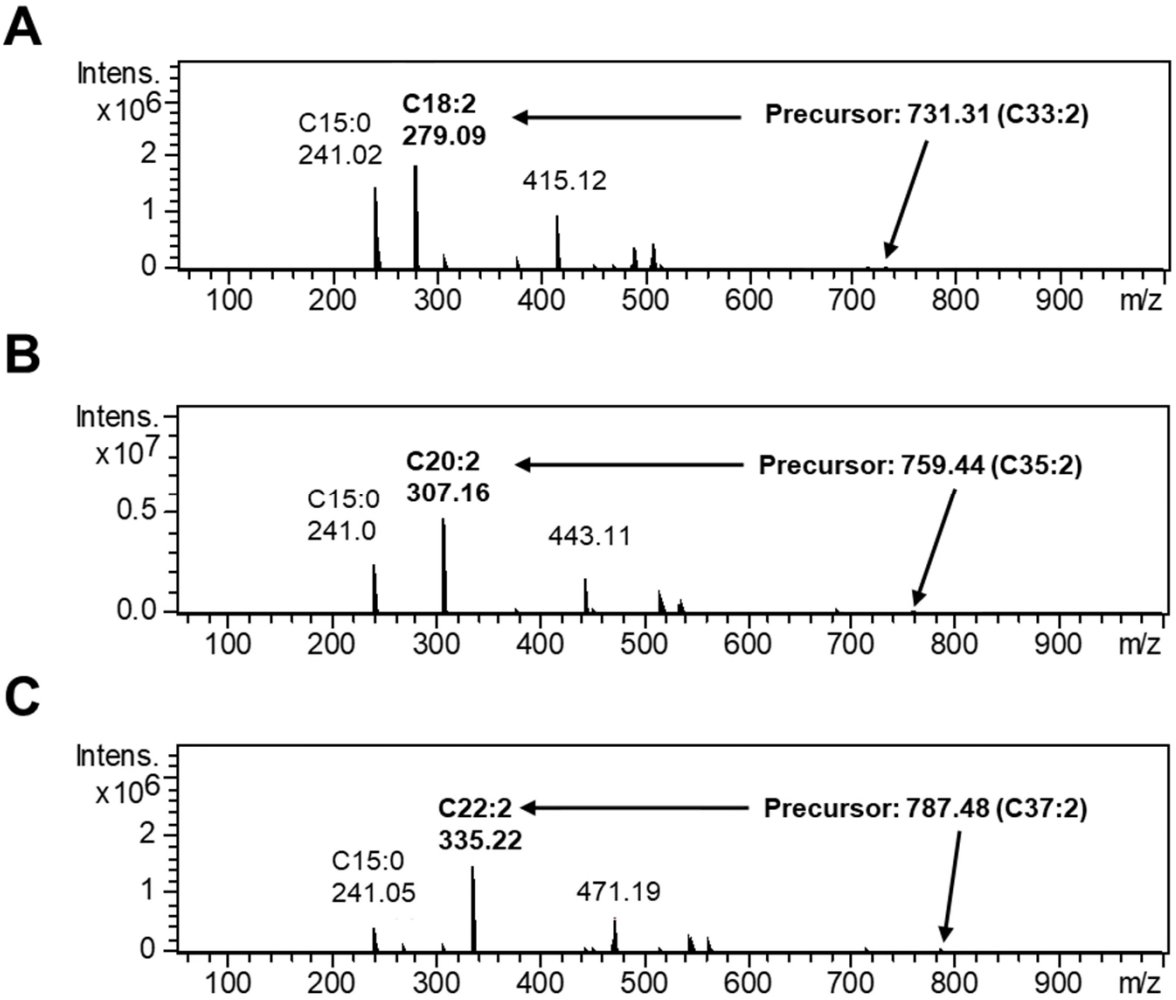
A
Intens.
x10^6
C15:0
241.02
C18:2
279.09
415.12
Precursor: 731.31 (C33:2)
B
Intens.
x10^7
C15:0
241.0
C20:2
307.16
443.11
Precursor: 759.44 (C35:2)
C
Intens.
x10^6
C15:0
241.05
C22:2
335.22
471.19
Precursor: 787.48 (C37:2)
m/z

Fig. S4

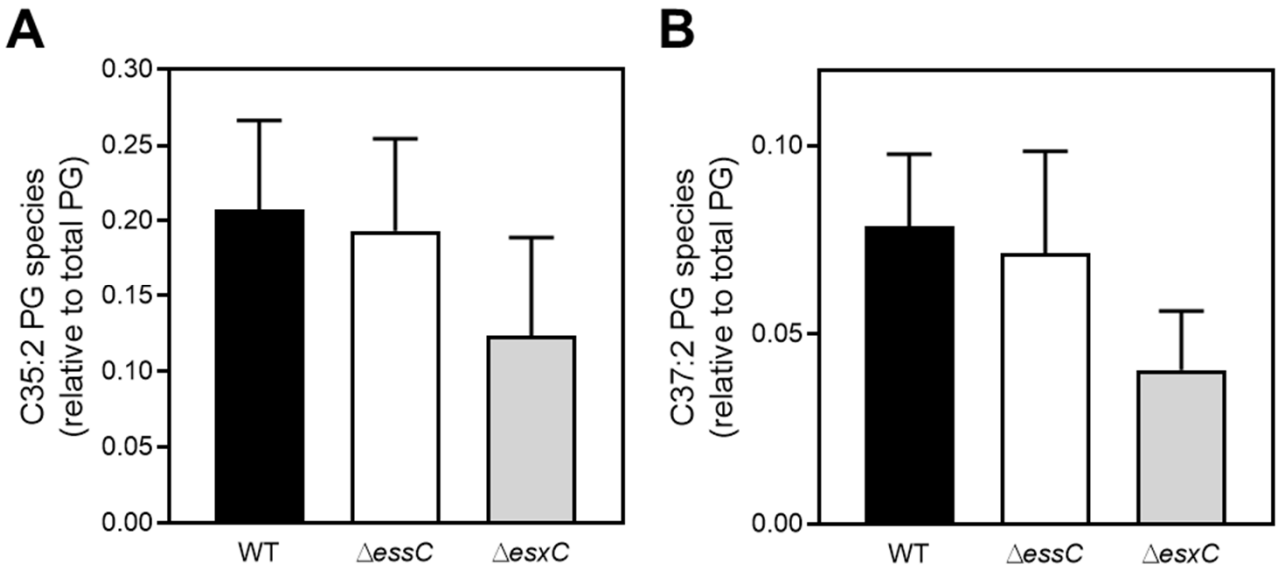
A
C35:2 PG species
(relative to total PG)
0.30
0.25
0.20
0.15
0.10
0.05
0.00
WT
ΔessC
ΔesxC
B
C37:2 PG species
(relative to total PG)
0.10
0.05
0.00
WT
ΔessC
ΔesxC

Fig. S5

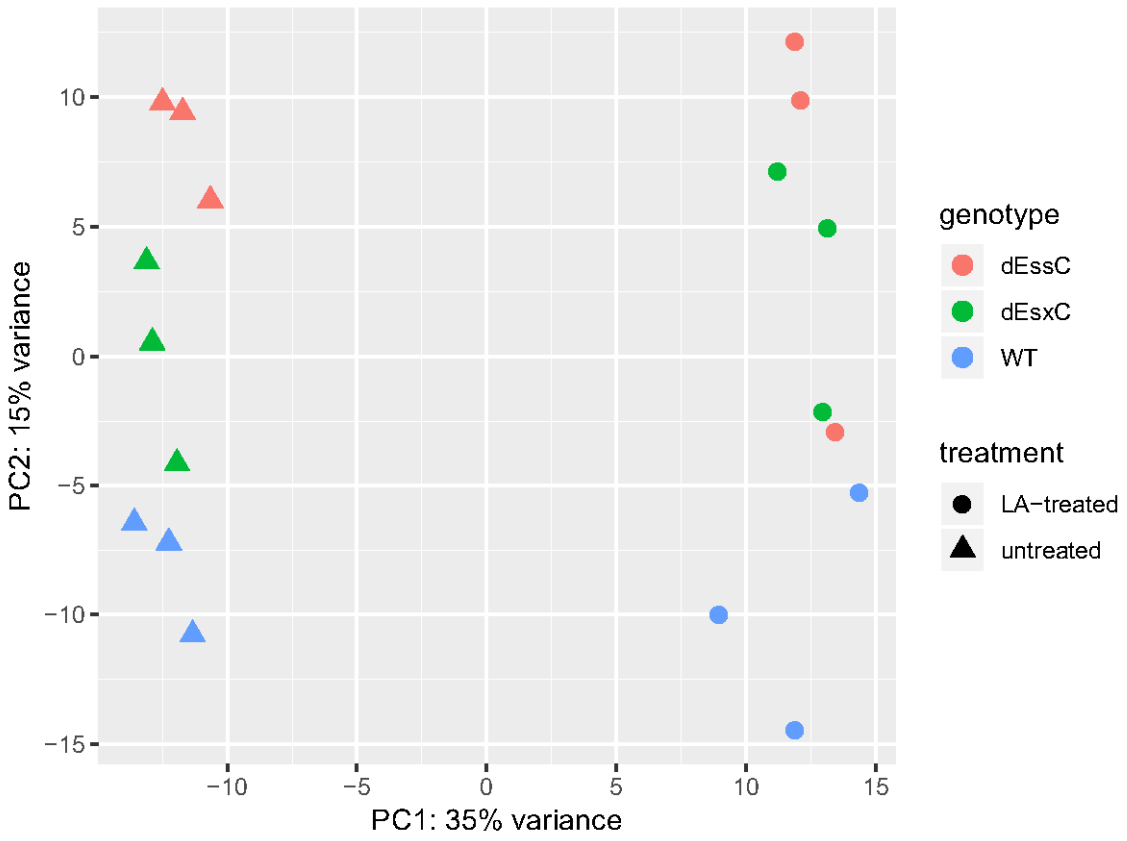
PC2: 15% variance
PC1: 35% variance
10
5
0
−5
−10
−15
−10
−5
0
5
10
15
genotype
dEssC
dEsxC
WT
treatment
LA−treated
untreated

Fig. S6

A

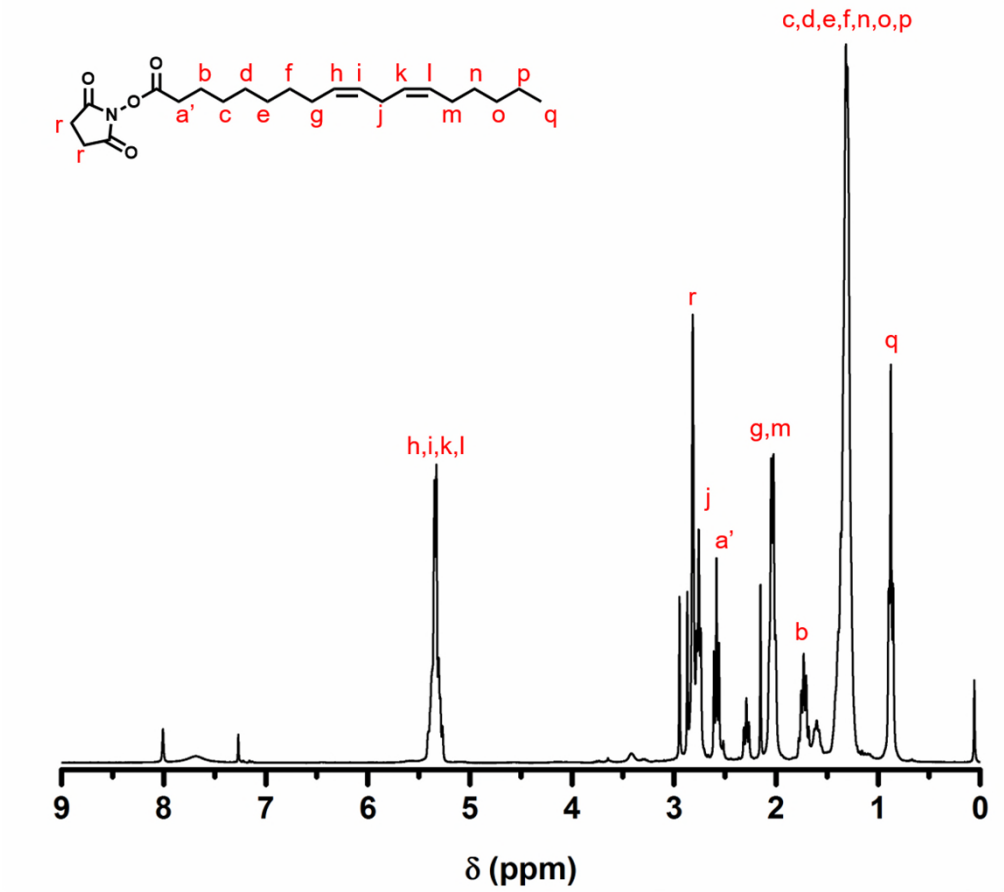
c,d,e,f,n,o,p
r
q
g,m
h,i,k,l
j
a'
b
9 8 7 6 5 4 3 2 1 0
δ (ppm)

B

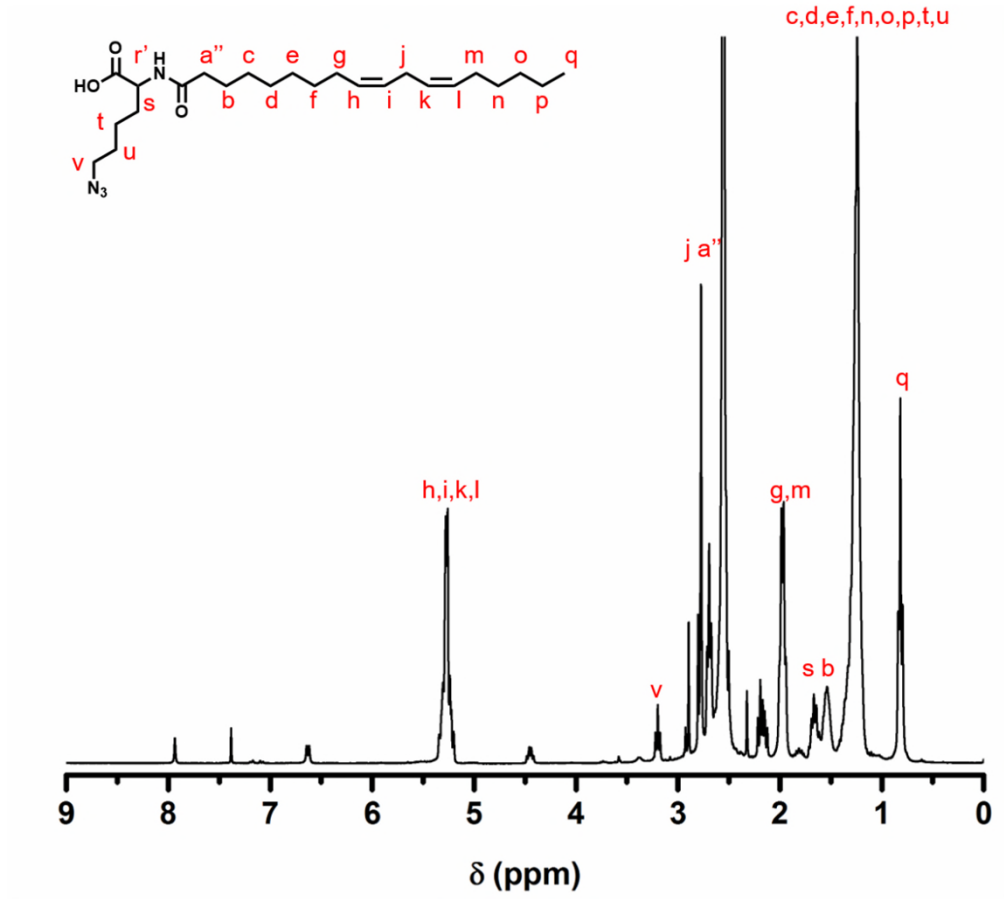
c,d,e,f,n,o,p,t,u
j a''
q
h,i,k,l
g,m
s b
v
9 8 7 6 5 4 3 2 1 0
δ (ppm)

Fig. S7